

# Petrogenesis of acapulcoites and lodranites: A shock-melting model

Alan E. Rubin \*

*Institute of Geophysics and Planetary Physics, University of California, Los Angeles, CA 90095-1567, USA*

Received 31 May 2006; accepted in revised form 20 February 2007; available online 23 February 2007

## Abstract

Acapulcoites are modeled as having formed by shock melting CR-like carbonaceous chondrite precursors; the degree of melting of some acapulcoites was low enough to allow the preservation of 3–6 vol % relict chondrules. Shock effects in acapulcoites include veins of metallic Fe–Ni and troilite, polycrystalline kamacite, fine-grained metal–troilite assemblages, metallic Cu, and irregularly shaped troilite grains within metallic Fe–Ni. While at elevated temperatures, acapulcoites experienced appreciable reduction. Because graphite is present in some acapulcoites and lodranites, it seems likely that carbon was the principal reducing agent. Reduction is responsible for the low contents of olivine Fa (4–14 mol %) and low-Ca pyroxene Fs (3–13 mol %) in the acapulcoites, the observation that, in more than two-thirds of the acapulcoites, the Fa value is lower than the Fs value (in contrast to the case for equilibrated ordinary chondrites), the low FeO/MnO ratios in acapulcoite olivine (16–18, compared to 32–38 in equilibrated H chondrites), the relatively high modal orthopyroxene/olivine ratios (e.g., 1.7 in Monument Draw compared to 0.74 in H chondrites), and reverse zoning in some mafic silicate grains. Lodranites formed in a similar manner to acapulcoites but suffered more extensive heating, loss of plagioclase, and loss of an Fe–Ni–S melt.

Acapulcoites and lodranites experienced moderate post-shock annealing, presumably resulting from burial beneath material of low thermal diffusivity. The annealing process repaired damaged olivine crystal lattices, lending acapulcoites and lodranites the appearance of unshocked (i.e., shock-stage S1) rocks. Any high-pressure phases that may have formed during initial shock reverted to their low-pressure polymorphs during annealing. Some samples were subsequently shocked again; several acapulcoites reached shock-stage S2 levels, ALH 84190 reached S3, and the lodranite MAC 88177 reached S5.

© 2007 Elsevier Ltd. All rights reserved.

## 1. INTRODUCTION

Acapulcoites and lodranites constitute two related groups of “primitive achondrites” (e.g., Prinz et al., 1980, 1983; Kimura et al., 1992) that possess recrystallized textures, chondritic mineralogy, approximately chondritic bulk compositions and overlapping O-isotopic compositions (similar to those in CR carbonaceous chondrites; Clayton and Mayeda, 1996, 1999). Lodranites differ from acapulcoites in being coarser grained and in having subchondritic proportions of troilite and/or plagioclase. The two groups are widely considered to have formed by incomplete melting of chondritic

material (e.g., Palme et al., 1981; Nagahara, 1992; Zipfel et al., 1995; McCoy et al., 1996, 1997a,b; Mittlefehldt et al., 1996; Patzer et al., 2004). Although Kallemeyn and Wasson (1985) suggested that the acapulcoites were heated during collisions on their parent asteroid, McCoy et al. (1996) ruled out this mechanism because acapulcoite olivine grains typically exhibit either sharp optical extinction or undulose extinction (without associated planar fractures), characteristic of unshocked or very weakly shocked rocks. Alternative heating mechanisms (e.g., electromagnetic induction or  $^{26}\text{Al}$  decay) for the primitive achondrites were deemed more plausible (Zipfel et al., 1995; McCoy et al., 1996) than impact-induced heating.

However, because it is possible that post-shock annealing processes could heal the damaged olivine crystal lattices in asteroidal materials and make the samples appear less

\* Fax: +1 310 206 3051.

E-mail address: [aerubin@ucla.edu](mailto:aerubin@ucla.edu)

shocked than they once were (Rubin, 2002, 2003; Rubin and Jones, 2003), it seemed worthwhile to search for relict shock features in acapulcoites and lodranites.

Post-shock annealing processes have been invoked previously for other meteorite groups. Rubin (2004) studied 210 equilibrated ordinary chondrites (OC) of shock stages S1 and S2 and identified numerous petrographic characteristics as being relict shock features (including curvilinear trails of metal and sulfide blebs within silicate grains, chromite veinlets within silicate grains, chromite–plagioclase assemblages, polycrystalline troilite, metallic Cu, metal–sulfide veins, and irregularly shaped troilite grains within metallic Fe–Ni). He concluded that these OC were shocked, insulated by impact-comminuted materials, and annealed. CK chondrites (Rubin, 1992), EL chondrites (Rubin et al., 1997) and ureilites (Rubin, 2006) may have experienced broadly similar shock and annealing histories.

## 2. ANALYTICAL PROCEDURES

Thin sections of eight acapulcoites and four lodranites (Table 1) were examined microscopically in transmitted and reflected light. Grain sizes were measured microscopically using a calibrated reticle. The modal abundances of phases were measured microscopically at 500× in reflected light with an automated Swift/Prior point counting system using a step interval of 220 μm. Chromite and silicate compositions were determined with the JEOL JXA-8200 electron microprobe at UCLA using a focused beam, natural and synthetic standards, an accelerating voltage of 15 keV, a 15 nA sample current, 20 s counting times per element, and ZAF corrections. Silicate phases containing opaque clusters were identified by EDS and by quantitative analyses using the JEOL electron microprobe.

## 3. RESULTS

### 3.1. Relict chondrules

Relict chondrules are present in acapulcoites. Yanai and Kojima (1991) identified poorly defined, highly recrystal-

lized ~250-μm-size barred olivine (BO) chondrules in Y 74063. McCoy et al. (1996) reported a single 1300 × 1900-μm-size relict radial pyroxene (RP) chondrule in Monument Draw.

There are additional examples of relict chondrules in two other acapulcoites—GRA 98028 and Dhofar 1222 (Fig. 1). The original mean chondrule sizes in these rocks are likely to be smaller than indicated below because small relict chondrules are difficult to distinguish from coarse mafic silicate grains in the groundmass. For the same reason, the proportion of relict chondrules given here should be considered a lower limit.

GRA 98028 contains ~6 vol % relict chondrules ranging in apparent diameter from 400 to 700 μm. Chondrule types include porphyritic olivine-pyroxene (POP, e.g., Fig. 1a) and porphyritic pyroxene (PP). Phenocryst grain sizes range from 15 to 80 μm. Many phenocrysts contain 15- to 20-μm-long curvilinear trails of 2- to 8-μm-size blebs of metallic Fe–Ni and troilite.

Dhofar 1222 contains ~4 vol % relict chondrules ranging in apparent diameter from 300 to 1400 μm and averaging ~700 μm. Chondrule types include RP (e.g., Fig. 1b), GOP (granular olivine-pyroxene) and PO (porphyritic olivine). The largest chondrule is a 1400-μm, quasi-equant RP chondrule.

There are no known examples of relict chondrules in lodranites.

### 3.2. Shock stages

Following the criteria of Stöffler et al. (1991), shock stages were assigned to the acapulcoites and lodranites in this study (Table 1). Most acapulcoites are shock-stage S1 or S2. Although McCoy et al. (1996) classified ALH 84190 as S2, its olivine grains exhibit undulose extinction and contain planar fractures; it is classified here as S3. The rock also exhibits moderate silicate darkening (a characteristic attributed to shock by Heymann, 1967; Britt and Pieters, 1991, and Rubin, 1992): every silicate grain in ALH 84190 is traversed by 50- to 150-μm-long curvilinear trails of 0.2- to 2-μm-size metal and troilite blebs.

Table 1  
Thin sections examined in the current study

| Meteorite              | Sections  | Classification | Shock stage |
|------------------------|-----------|----------------|-------------|
| ALH A77081             | 17        | Acapulcoite    | S1          |
| ALH 84190              | 8         | Acapulcoite    | S3          |
| Dhofar 1222            | UCLA 1865 | Acapulcoite    | S2          |
| GRA 98028              | 4 and 31  | Acapulcoite    | S1          |
| LEW 86220              | 2 and 5   | Acapulcoite    | S2          |
| MET 01195 <sup>a</sup> | 13        | Acapulcoite    | S1          |
| MET 01212 <sup>a</sup> | 8         | Acapulcoite    | S1          |
| Superior Valley 014    | UCLA 1851 | Acapulcoite    | S2          |
| EET 84302 <sup>b</sup> | 28        | Lodranite      | S1          |
| GRA 95209              | 41 and 45 | Lodranite      | S1          |
| LEW 88280              | 11        | Lodranite      | S1          |
| MAC 88177              | 16 and 48 | Lodranite      | S5          |

Antarctic sections from NASA Johnson Space Center; Dhofar and Superior Valley sections from UCLA.

<sup>a</sup> MET 01195 and MET 01212 are probably paired.

<sup>b</sup> EET 84302 is transitional between acapulcoites and lodranites (McCoy et al., 1993). It is classified as a lodranite by Grady (2000), but considered more closely related to acapulcoites by Mittlefehldt et al. (1996).

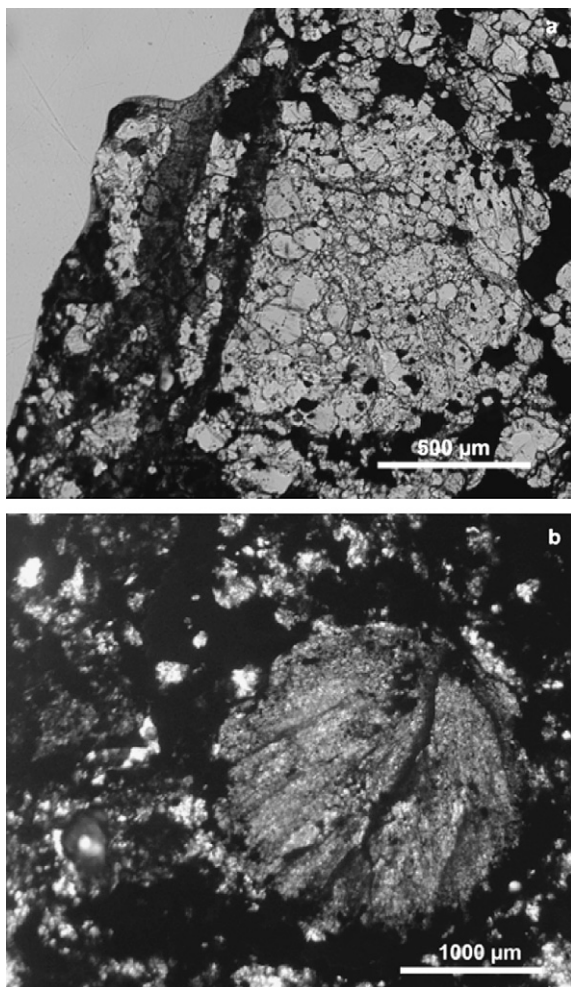


Fig. 1. Relict chondrules in acapulcoites. (a) Relict, fragmented POP chondrule in GRA 98028. (b) Relict RP chondrule in Dhofar 1222. Both images in transmitted light.

Three of the four lodranites in this study are S1. The MAC 88177 lodranite is appreciably more shocked. It contains olivine and pyroxene grains exhibiting strong mosaicism indicative of shock-stage S5. The meteorite contains several fine-grained metal–troilite assemblages (characterized as rapidly solidified assemblages by Scott, 1982 and attributed to shock heating and quenching). Also present are a few dark veins that include small grains of metal and sulfide. Rubin et al. (2002) reported low-Ca clinopyroxene (i.e., clinobronzite, not pigeonite) in this rock; this phase forms by quenching of either protoenstatite or high-temperature clinoenstatite and can be a shock indicator (e.g., Hornemann and Müller, 1971; Stöffler et al., 1991; Rubin et al., 1997).

### 3.3. Opaque phases

#### 3.3.1. General features

Acapulcoites vary significantly in their modal abundances of metallic Fe–Ni and troilite (Table 2). Those rocks containing abundant relict chondrules (GRA 98028; Dhofar 1222)

have greater abundances of opaque phases (30–40 wt%, e.g., Fig. 2a) than typical acapulcoites (13–20 wt%, e.g., Fig. 2b). Also containing abundant opaques (~40 wt%) is LEW 86220, which is texturally intermediate between acapulcoites and lodranites (McCoy et al., 1996, 1997b) and is relict-chondrule free. Most acapulcoites contain 4–7 wt% troilite, similar to the abundances in OC falls (5–6 wt%; Jarosewich, 1990); however, the relict-chondrule-bearing GRA 98028 contains a higher troilite abundance (18.5 wt%). Whereas typical acapulcoites have metal/troilite weight ratios of 1.4–2.4, Dhofar 1222 has a ratio of 4.3, and LEW 86220 has a ratio of 6.1. (Precise metal/troilite weight ratios could not be determined in GRA 98028 because of the high abundance of limonite in this weathered sample.)

Metal grains are typically irregular in shape; some are elongated, others are quasi-equant. Many are embayed by silicate grains (Fig. 2). (Similar metal–silicate textures are present in rare metal-bearing terrestrial basalts, indicating that the metal in these rocks was probably once molten; Fig. 309 of Ramdohr, 1980.) Metal grains in ALH 84190 average ~120 μm in mean size, those in ALH A77081, GRA 98028 and MET 01195 average ~200 μm, and those in Dhofar 1222 and LEW 86220 average ~400 μm; many metal grains in LEW 86220 (which is texturally intermediate between acapulcoites and lodranites) exceed 1000 μm. Petrographic examination of nitric-acid-etched sections indicates that most metal grains in acapulcoites are predominantly kamacite; a few grains contain several percent 10- to 40-μm-size patches of taenite. Between 30% and 60% of the metal grains are adjacent to troilite; however, most of the troilite grains are isolated and average ~100 μm in mean size.

Chromite abundances in acapulcoites vary from <0.05 wt% in LEW 86220 to 1.7 wt% in ALH A77081. A large (150 × 300 μm) subhedral chromite grain attached to metal and troilite occurs in MET 01195. Even larger (≥1.5 mm) elongated clusters of separate chromite grains are also present (Fig. 3). Smaller chromite grains occur in ALH A77081, Dhofar 1222 and GRA 98028.

Lodranites typically contain coarser metal grains (e.g., averaging ~1 mm in EET 84302) than acapulcoites (e.g., Fig. 2c). Their metal/troilite ratios tend to be greater than those in typical acapulcoites (Table 2); the ratio in EET 84302 is ~430. In contrast, the shock-stage S5 lodranite MAC 88177 has a metal/troilite ratio of only 0.6. This rock also contains smaller metal grains (averaging ~200 μm) than other lodranites (Fig. 2d). The total abundance of metal and troilite in MAC 88177 (7 wt%) is much lower than that of any other lodranite or acapulcoite (except the highly weathered acapulcoite Superior Valley 014).

Graphite occurs in several characteristic morphologies within a few metal grains of some acapulcoites and lodranites. Palme et al. (1981) and Schultz et al. (1982) reported graphite in Acapulco and ALH A77081; El Goresy et al. (2005, and references therein) made extensive studies of acapulcoite graphite. I have adopted the terminology of El Goresy et al. (2005) for the textural types of graphite reported here. The MET 01195 acapulcoite contains several metal grains with 30- to 150-μm-size graphite spherulites and adjacent branching graphite books (e.g., Fig. 4a). The V-shaped books are typically 4–10 μm thick and

Table 2  
Modal abundances of phases in acapulcoites and lodranites

| Meteorite      | ALH A77081  |      | ALH 84190   |      | Dhofar 1222 |      | GRA 98028   |                  | LEW 86220   |       | MET 01195   |       |
|----------------|-------------|------|-------------|------|-------------|------|-------------|------------------|-------------|-------|-------------|-------|
| Section        | 17          |      | 8           |      | UCLA 1865   |      | 4           |                  | 5           |       | 13          |       |
| Group          | acapulcoite |      | acapulcoite |      | acapulcoite |      | acapulcoite |                  | acapulcoite |       | acapulcoite |       |
| No. of points  | 543         |      | 1242        |      | 2235        |      | 1498        |                  | 2089        |       | 1508        |       |
|                | vol %       | wt%              | vol %       | wt%   | vol %       | wt%   |
| Silicate       | 88.2        | 80.4 | 89.4        | 82.7 | 73.8        | 57.6 | 69.1        | 57.9             | 76.4        | 59.5  | 85.5        | 76.3  |
| Kamacite       | 4.4         | 9.8  | 3.9         | 8.8  | 16.2        | 31.0 | 6.1         | 12.5             | 17.8        | 34.0  | 5.8         | 12.7  |
| Taenite        | 0.0         | 0.0  | 0.0         | 0.0  | 0.3         | 0.6  | 0.0         | 0.0              | 0.0         | 0.0   | 0.0         | 0.0   |
| Troilite       | 5.2         | 6.9  | 2.7         | 3.6  | 6.4         | 7.3  | 15.1        | 18.5             | 4.9         | 5.6   | 4.9         | 6.4   |
| Chromite       | 1.3         | 1.7  | 0.0         | 0.0  | 0.0         | 0.3  | 0.3         | 0.4              | 0.0         | 0.0   | 0.7         | 0.9   |
| Graphite       | 0.0         | 0.0  | 0.0         | 0.0  | 0.0         | 0.0  | 0.0         | 0.0              | 0.0         | 0.0   | 0.1         | 0.1   |
| Metallic Cu    | 0.0         | 0.0  | 0.0         | 0.0  | 0.0         | 0.0  | 0.0         | 0.0              | 0.0         | 0.0   | 0.0         | 0.0   |
| Limonite       | 0.9         | 1.1  | 3.9         | 4.8  | 3.0         | 3.1  | 9.5         | 10.7             | 0.9         | 0.9   | 3.0         | 3.6   |
| Total          | 100.0       | 99.9 | 99.9        | 99.9 | 100.0       | 99.9 | 100.1       | 100.0            | 100.0       | 100.0 | 100.0       | 100.0 |
| Metal/troilite |             | 1.4  |             | 2.4  |             | 4.3  |             | 0.7 <sup>a</sup> |             | 6.1   |             | 2.0   |

| Meteorite      | Superior Valley 014 |      | EET 84302 |       | GRA 95209 <sup>b</sup> |       | LEW 88280 |       | MAC 88177 |       |
|----------------|---------------------|------|-----------|-------|------------------------|-------|-----------|-------|-----------|-------|
| Section        | UCLA 1851           |      | 28        |       | 45                     |       | 11        |       | 16        |       |
| Group          | acapulcoite         |      | lodranite |       | lodranite              |       | lodranite |       | lodranite |       |
| No. of points  | 1559                |      | 2252      |       | 3717                   |       | 1051      |       | 2261      |       |
|                | vol %               | wt%  | vol %     | wt%   | vol %                  | wt%   | vol %     | wt%   | vol %     | wt%   |
| Silicate       | 82.8                | 77.8 | 74.8      | 55.4  | 64.6                   | 45.5  | 87.4      | 76.6  | 93.8      | 90.4  |
| Kamacite       | 0.1                 | 0.2  | 23.4      | 42.5  | 27.6                   | 47.7  | 8.5       | 18.3  | 1.1       | 2.6   |
| Taenite        | 0.0                 | 0.0  | 0.4       | 0.8   | 0.0                    | 0.1   | 0.0       | 0.0   | 0.0       | 0.0   |
| Troilite       | 2.5                 | 3.4  | 0.1       | 0.1   | 1.2                    | 1.2   | 3.0       | 3.8   | 3.1       | 4.4   |
| Chromite       | 0.1                 | 0.1  | 0.0       | 0.0   | 0.0                    | 0.0   | 0.2       | 0.3   | 0.7       | 1.0   |
| Graphite       | 0.0                 | 0.0  | 0.0       | 0.0   | 1.3                    | 0.6   | 0.0       | 0.0   | 0.0       | 0.0   |
| Metallic Cu    | 0.0                 | 0.0  | 0.0       | 0.0   | 0.0                    | 0.0   | 0.0       | 0.0   | 0.0       | 0.0   |
| Limonite       | 14.6                | 18.4 | 1.3       | 1.3   | 5.2                    | 4.9   | 0.9       | 1.0   | 1.3       | 1.7   |
| Total          | 100.1               | 99.9 | 100.0     | 100.1 | 99.9                   | 100.0 | 100.0     | 100.0 | 100.0     | 100.1 |
| Metal/troilite |                     | 0.1  |           | 430   |                        | 40    |           | 4.8   |           | 0.6   |

Weight-percent was determined from vol % using the following mineral densities ( $\text{g cm}^{-3}$ ): silicate (3.2), kamacite (7.85), taenite (8.19), troilite (4.67), chromite (4.7), graphite (2.2), metallic Cu (8.95), limonite (4.28). Modal abundances of 0.0 vol % imply an abundance of <0.05 vol %, not necessarily the absence of a phase.

<sup>a</sup> Ratios uncertain because of abundant limonite.

20–60  $\mu\text{m}$  long. The lodranite GRA 95209 contains a large (1020  $\times$  1340  $\mu\text{m}$ ) fan-shaped graphite spherulite within a very large (3.6  $\times$  6.8 mm) grain of metallic Fe–Ni (Fig. 4b). Smaller graphite spherulites also occur in the metallic Fe–Ni grain around the large graphite spherulite. Graphite exsolution veneers connect some of the smaller spherulites and indicate that the host metal grain is polycrystalline.

The terrestrially weathered acapulcoite and lodranite finds contain limonite patches that have replaced metal and troilite grains; also present in these rocks are thin limonite veins that traverse and fill fractures in silicate grains.

### 3.3.2. Veins of metallic Fe–Ni and troilite in acapulcoites

GRA 98028 contains thin ( $\sim$ 0.2- $\mu\text{m}$ -thick) curvilinear, branching, metal veins ranging in length from 50 to 200  $\mu\text{m}$ . LEW 86220 contains numerous 10- $\mu\text{m}$ -thick metal–troilite veins that exceed 100  $\mu\text{m}$  in length (Fig. 5a). In addition, a few millimeter-long veins of metal (and minor sulfide) transect the silicates in LEW 86220 and connect coarse metal grains.

Numerous troilite veins occur in ALH 84190 at silicate–silicate grain boundaries. ALH A77081 contains many 0.5- to 2- $\mu\text{m}$ -thick troilite veins that trace grain boundaries (silicate–silicate; metal–silicate) throughout the rock; the veins also transect many individual silicate grains. Some of the troilite veins contain small patches of metallic Fe–Ni. Thin sulfide veins also occur in LEW 86220 (Fig. 5b).

### 3.3.3. Polycrystalline kamacite in acapulcoites

McCoy et al. (1996) reported polycrystalline kamacite in all the acapulcoites that they studied. The most conspicuous occurrences are in ALH 84190 (the most shocked acapulcoite in this study; Table 1) wherein  $\sim$ 50% of the kamacite grains are polycrystalline. The kamacite–kamacite grain boundaries in these assemblages are sharp. Some polycrystalline kamacite assemblages consist of a single large grain (ca. 80–200  $\mu\text{m}$ ) and one or two small grains ( $\sim$ 20–50  $\mu\text{m}$ ) located at the margins; other polycrystalline kamacite assemblages contain multiple grains ranging from 25 to 90  $\mu\text{m}$  in size. In some cases, small taenite grains occur at kamacite–kamacite grain boundaries.

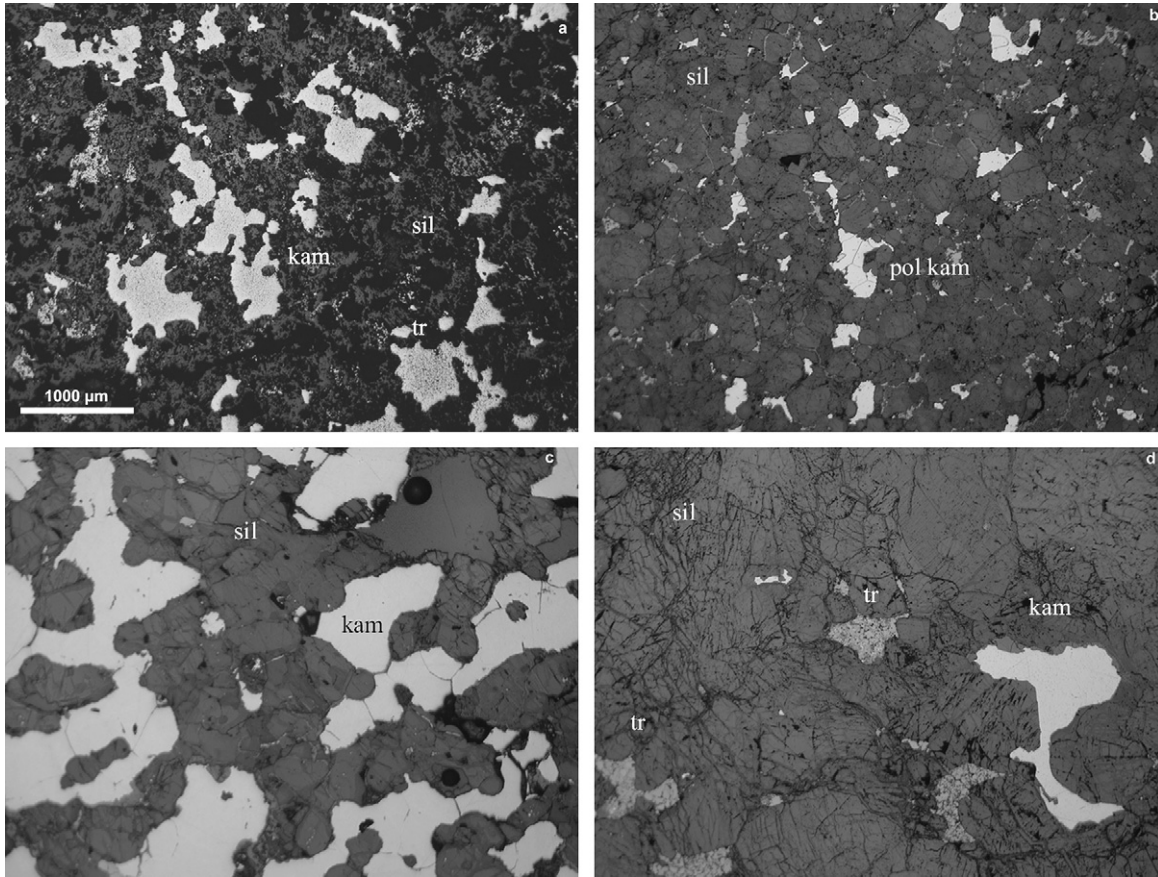


Fig. 2. Examples of textures and abundances of opaque phases in acapulcoites and lodranites. (a) Typical metal-rich region of acapulcoite Dhofar 1222. (b) Typical metal-poor region of acapulcoite ALH 84190. The central metal grain is polycrystalline kamacite. (c) Typical metal-rich region of lodranite GRA 95209. (d) Typical metal-poor region of lodranite MAC 88177. sil, silicate; tr, troilite; kam, kamacite; pol, polycrystalline. All images in reflected light. All images are at the same scale.

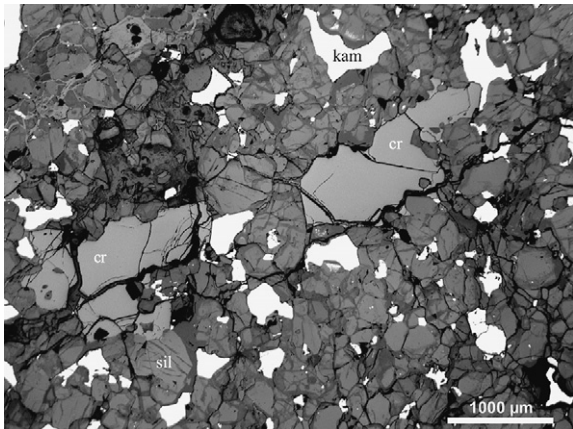


Fig. 3. Elongated clusters of separate chromite grains in acapulcoite MET 01195. Granular texture of silicates is also evident. sil, silicate; cr, chromite; kam, kamacite. Reflected light.

### 3.3.4. Fine-grained metal–troilite assemblages

ALH 84190 (shock-stage S3) contains several fine-grained metal–troilite assemblages (e.g., Fig. 6a). One 90- $\mu\text{m}$ -size metallic Fe–Ni grain in ALH 84190 contains an

18  $\times$  35  $\mu\text{m}$  ellipsoidal assemblage that consists of troilite containing  $\sim 15$  vol % 1- to 4- $\mu\text{m}$ -size metal blebs, close to the eutectic troilite/metal weight ratio of 7.5:1 (Brandes and Brook, 1998). The troilite grain is polycrystalline. Another fine-grained metal–troilite assemblage in this meteorite consists of  $\sim 95$  vol % metal and  $\sim 5$  vol % troilite; the troilite forms thin films that outline 6- to 18- $\mu\text{m}$ -diameter metal cells.

Fine-grained metal–troilite assemblages also occur in ALH A77081 (shock-stage S1). One 30  $\times$  65  $\mu\text{m}$  troilite grain contains  $\sim 30$  vol % metal cells that are 3–6  $\mu\text{m}$  in diameter.

The shock-stage S5 lodranite, MAC 88177, contains several fine-grained metal–troilite assemblages that appear to have undergone mechanical abrasion and, near their edges, low-degree melting, mixing and rapid solidification. In many cases, these regions occur at the edges of large troilite grains (e.g., Fig. 6b).

### 3.3.5. Irregular troilite grains in metallic Fe–Ni in acapulcoites

A few irregularly shaped troilite grains within metallic Fe–Ni occur in acapulcoites. GRA 98028 contains a coarse metal grain that includes a 10- $\mu\text{m}$ -wide patch of troilite

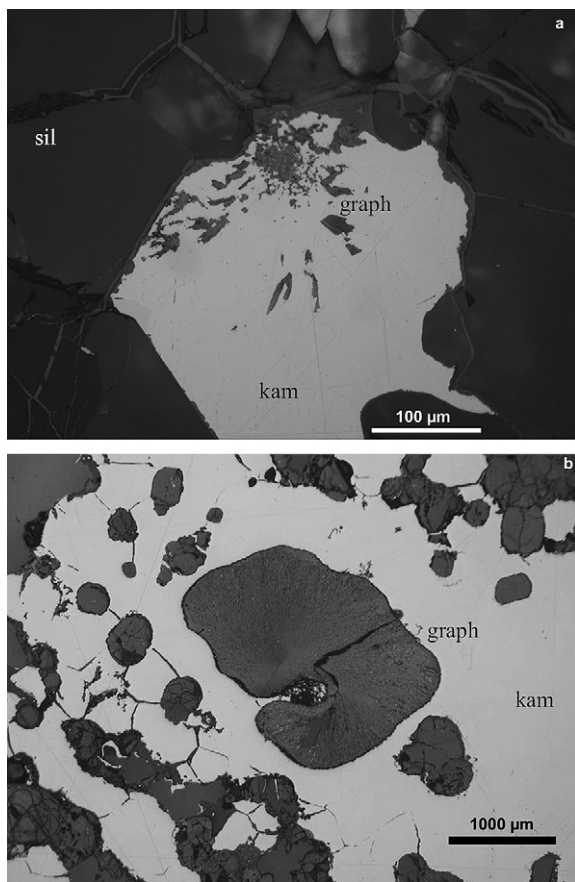


Fig. 4. Graphite in acapulcoites and lodranites. (a) Fine-grained graphite spherulite (top) and small, branching graphite books inside a metallic Fe–Ni grain in acapulcoite MET 01195. (b) A large spherulitic graphite and smaller satellite graphite spherulites in a very large metallic Fe–Ni grain in lodranite GRA 95209. Dark lines outlining metal grains are graphite exsolution veneers. sil, silicate; graph, graphite; kam, kamacite. Both images in reflected light.

consisting of  $\sim 4\text{-}\mu\text{m}$ -thick bands with ellipsoidal patches of metal between them (Fig. 7a). MET 01195 has a large ( $130 \times 240\ \mu\text{m}$ ) metal grain that contains a troilite grain at one edge that has a protrusion that forms an irregular  $\sim 10\text{-}\mu\text{m}$ -wide patch (Fig. 7b). Because mechanically deformed iron sulfide should show stress-induced twin lamellae (e.g., Fig. 410a,b,e of Ramdohr, 1980), it seems likely that the troilite in the GRA 98028 and MET 01195 opaque assemblages was molten. LEW 86220 contains rare metal grains with 20- to  $40\text{-}\mu\text{m}$ -size irregular troilite patches that include a few volume percent of  $2\text{-}\mu\text{m}$ -size metal grains. This rock also contains several metal grains with coarse, curved patches of troilite that range from  $20 \times 120\ \mu\text{m}$  to  $20 \times 200\ \mu\text{m}$ .

### 3.3.6. Metallic Cu in acapulcoites

Rare grains of metallic Cu occur within metallic Fe–Ni in Dhofar 1222. There are two thin elongated ( $2\text{--}4\ \mu\text{m}$ )  $\times$  ( $30\text{--}50\ \mu\text{m}$ ) bands of metallic Cu lining the interface between metallic Fe–Ni and troilite in large opaque assemblages (e.g., Fig. 8). Another metallic Cu grain in this meteorite forms a  $4 \times 14\text{-}\mu\text{m}$ -size protrusion into

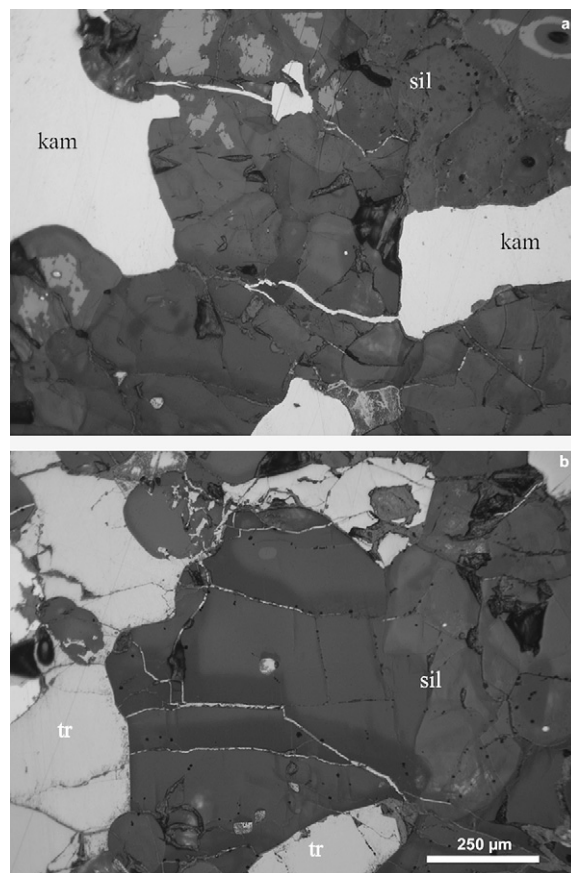


Fig. 5. Opaque veins in acapulcoites. (a) Thin metallic Fe–Ni veins extending from large metallic Fe–Ni grains in LEW 86220 and traversing adjacent silicates. (b) Thin fracture-filling troilite veins in LEW 86220. Illustrated regions are distant from the fusion crusts of these samples. sil, silicate; tr, troilite; kam, kamacite. Both images in reflected light and to the same scale.

metallic Fe–Ni from the interface with troilite. A third metallic Cu grain is  $\sim 3 \times 10\ \mu\text{m}$  in size and occurs at the kamacite/silicate boundary. These are the first metallic Cu grains to be reported in acapulcoites. No metallic Cu was observed in lodranites.

### 3.3.7. Opaque blebs in the centers of silicate grains

McCoy et al. (1996) reported that many silicate grains (particularly orthopyroxene) in acapulcoites contain ovoid clusters of small ( $5\text{--}10\ \mu\text{m}$ ) metal and troilite blebs in their centers. These textures were also reported by other workers (e.g., Palme et al., 1981; Zipfel et al., 1995; Mittlefehldt et al., 1996; El Goresy et al., 2005). My observations indicate that  $\sim 15\%$  of the silicate grains (olivine, low-Ca pyroxene and diopside) in ALH A77081,  $\sim 15\%$  in MET 01195, and  $\sim 25\%$  in GRA 98028 (Fig. 9a and b) have central regions that contain 2- to  $16\text{-}\mu\text{m}$ -size rounded and oblong blebs of metal, troilite, metal–troilite, chromite, chromite–troilite, and chromite–metal. These central regions are overgrown by inclusion-free silicate. Electron microprobe analysis indicates that the small chromite grains in these opaque clusters are appreciably depleted in  $\text{TiO}_2$  and  $\text{Al}_2\text{O}_3$ , and somewhat depleted in  $\text{MgO}$  relative

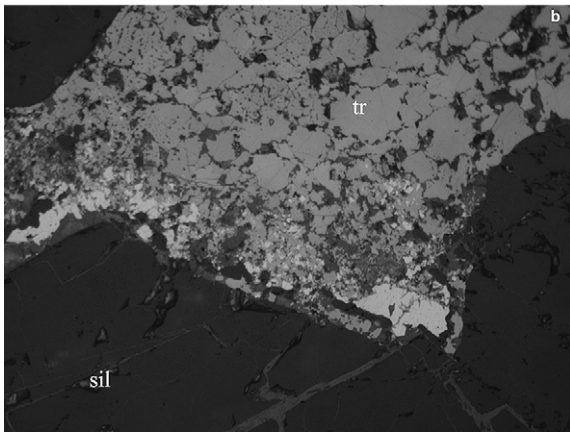
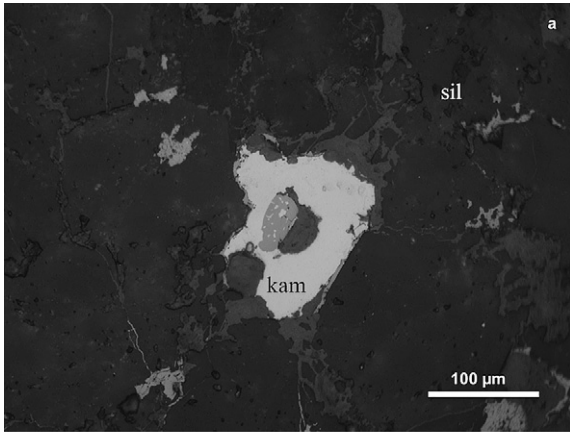


Fig. 6. Rapidly solidified metal–troilite assemblages. (a) Metal grain in acapulcoite ALH 84190 containing an ellipsoidal troilite grain with small metal blebs formed as a result of melting and quenching. (b) Edge of large troilite grain in lodranite MAC 88177 that consists of intergrown, rapidly solidified metal–sulfide. sil, silicate; tr, troilite; kam, kamacite. Both images in reflected light and to the same scale.

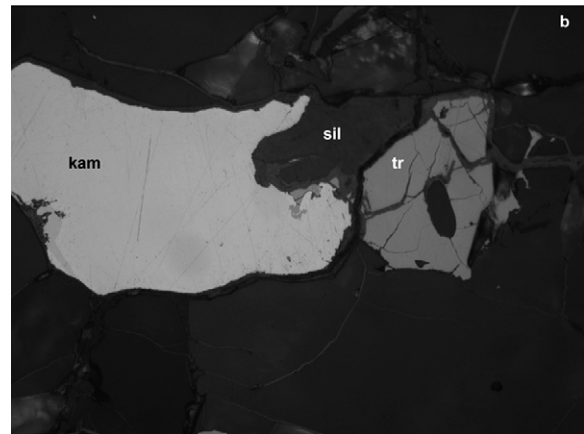
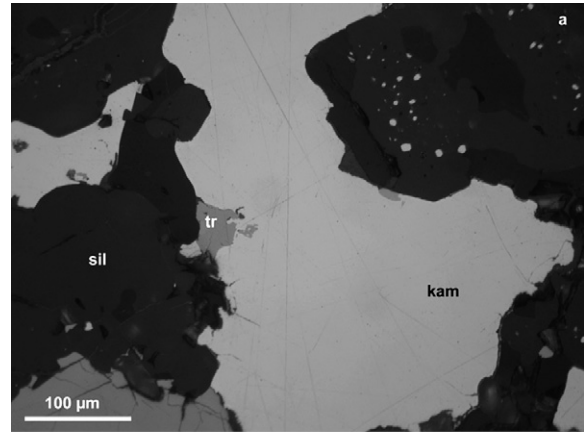


Fig. 7. Irregular troilite grains inside metallic Fe–Ni in two acapulcoites. (a) A large kamacite (kam) grain in GRA 98028 with an adjacent troilite (tr) grain contains small irregular appendages of troilite. (b) Small irregular troilite grains inside kamacite (kam) in MET 01195. sil, silicate. Both images in reflected light and to the same scale.

to coarser chromite grains in the matrix (Table 3). The small cluster chromite grains in GRA 98008 are also enriched in FeO relative to coarser chromite grains in the matrix of MET 01195.

Clusters of opaque grains also occur in lodranites. Approximately 10–15% of the mafic silicate grains in LEW 88280 (McCoy et al., 1997a) and GRA 95209 contain clusters of 2- to 25- $\mu\text{m}$ -size blebs of metal and metal–troilite. The clusters in LEW 88280 range from 20 to 40  $\mu\text{m}$ ; those in GRA 95209 range from 30 to 200  $\mu\text{m}$ .

A far higher abundance of clusters of opaque grains occurs in the EET 84302 lodranite;  $\sim$ 50% of the silicate grains in this rock contain ovoid, elongated, and quasi-equant clusters, 20  $\times$  40 to 70  $\times$  500  $\mu\text{m}$  in size, of rounded 2- to 14- $\mu\text{m}$ -size metal blebs. The clusters occupy very discrete regions in the silicate grains and are surrounded by clear, inclusion-free silicate (Fig. 9c and d).

### 3.4. Oxygen isotopic composition of Superior Valley 014

Acapulcoites and winonaites are groups of primitive achondrites of similar mineralogy and with similar recrystallized textures (e.g., Hutchison, 2004); the groups overlap in their olivine Fa distributions but have distinct ranges in

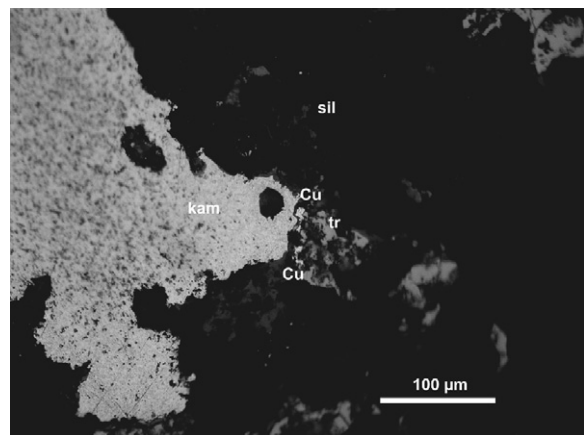


Fig. 8. Thin, elongated metallic Cu grain (Cu) lining the boundary between troilite (tr) and fine-grained polycrystalline kamacite (kam) in Dhofar 1222. sil, silicate. The speckled texture of the kamacite grain is a result of terrestrial weathering. Reflected light.

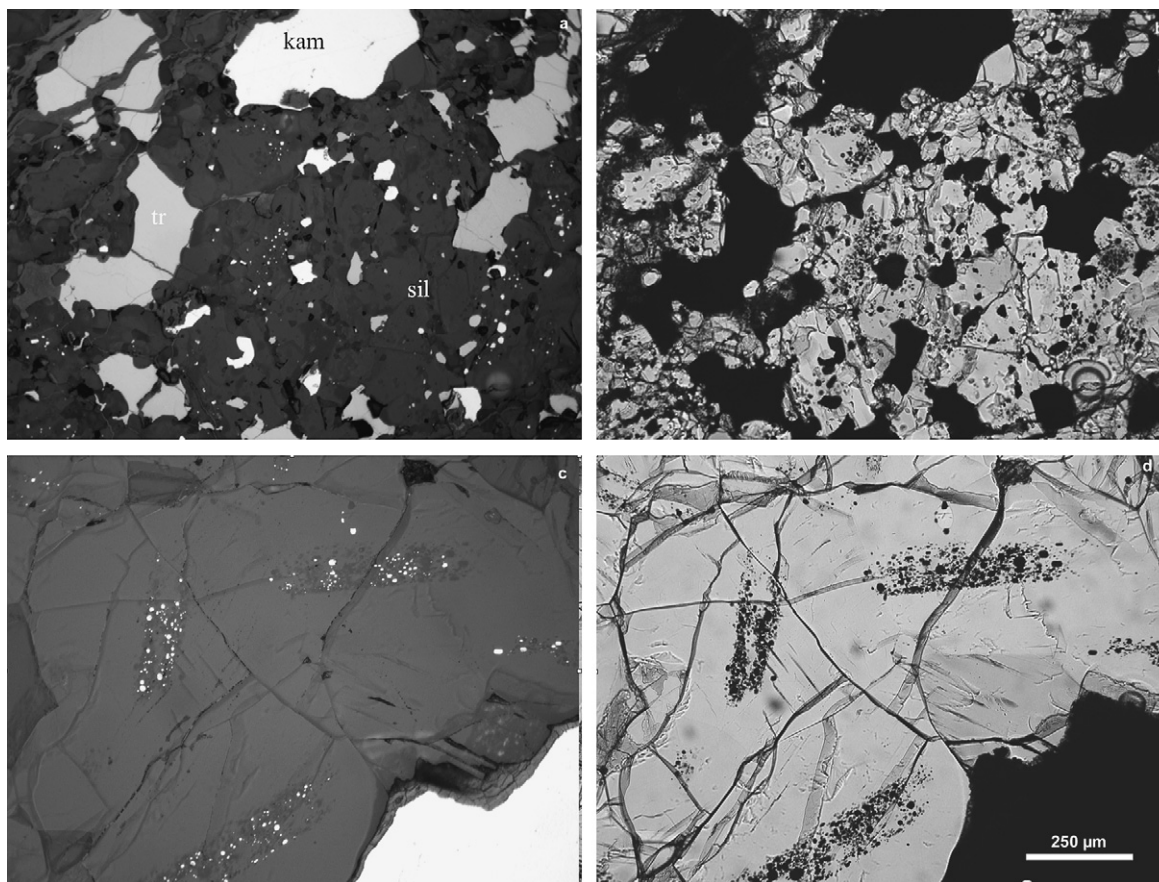


Fig. 9. Clusters of opaque grains in the centers of silicate grains in acapulcoites and lodranites. (a) Reflected light image of acapulcoite GRA 98028. In addition to coarse metal and troilite grains, there are some silicate grains (medium gray) containing clusters of small metal grains (white blebs) in their centers. (b) Same region as (a) in transmitted light. Opaques are black. (c) Reflected light image of well-defined clusters of metal and troilite grains (white) in the centers of silicate grains (medium gray) in lodranite EET 84302. (d) Same region as (c) in transmitted light. Clusters of opaques appear as concentrations of black blebs. sil, silicate; kam, kamacite; tr, troilite. All images to the same scale.

Table 3  
Mean chromite compositions (wt%) in two acapulcoites

| Meteorite                      | GRA 98028            | GRA 98028    | MET 01195     |
|--------------------------------|----------------------|--------------|---------------|
| Occurrence                     | Small cluster grains | Coarse grain | Coarse grains |
| No. of grains                  | 2                    | 1            | 5             |
| SiO <sub>2</sub>               | 0.28                 | 0.24         | 0.06          |
| TiO <sub>2</sub>               | 0.54                 | 0.90         | 1.2           |
| Al <sub>2</sub> O <sub>3</sub> | 3.1                  | 6.7          | 6.7           |
| Cr <sub>2</sub> O <sub>3</sub> | 64.8                 | 58.6         | 61.3          |
| FeO                            | 21.7                 | 22.2         | 18.0          |
| MnO                            | 1.6                  | 1.4          | 1.5           |
| MgO                            | 6.7                  | 7.2          | 9.3           |
| CaO                            | 0.12                 | 0.05         | 0.08          |
| Na <sub>2</sub> O              | 0.12                 | 0.13         | 0.11          |
| total                          | 99.0                 | 97.4         | 98.2          |

The low totals are probably due to the presence of some Fe<sub>2</sub>O<sub>3</sub>.

O-isotopic composition (Rumble et al., 2005). Superior Valley 014 (mean Fa = 4.6 mol %) is within the range of olivine composition for both acapulcoites and winonaites; the O-isotopic compositions of replicate samples of this meteorite (Table 4) were determined by an infrared-laser fluorination

technique following a modification of the procedures of Young et al. (1998). The mean  $\Delta^{17}\text{O}$  value of Superior Valley 014 is  $-1.04\text{‰}$  (Table 4; K. Ziegler, pers. commun., 2006). This value is well within the acapulcoite range ( $\Delta^{17}\text{O} = -0.85$  to  $-1.22\text{‰}$ ; Clayton and Mayeda, 1996)

Table 4  
Oxygen-isotopic composition of Superior Valley 014

| Sample | Mass (mg) | $\delta^{17}\text{O}$ (‰) | $\delta^{18}\text{O}$ (‰) | $\Delta^{17}\text{O}$ (‰) |
|--------|-----------|---------------------------|---------------------------|---------------------------|
| 1      | 2.16      | 1.05                      | 4.01                      | -1.07                     |
| 2      | 1.60      | 1.14                      | 4.08                      | -1.02                     |
|        | Mean      | 1.10                      | 4.04                      | -1.04                     |

and outside the winonaite range ( $\Delta^{17}\text{O} = \sim -0.4$  to  $-0.80\%$ ; Rumble et al., 2005). It is clear that Superior Valley 014 is an acapulcoite.

## 4. DISCUSSION

### 4.1. Nature of acapulcoite precursor material

There are four principal pieces of evidence that indicate that the precursors of acapulcoites were chondrites: (1) several acapulcoites contain relict chondrules; chondrule types include porphyritic, barred olivine, radial pyroxene and granular olivine-pyroxene. The acapulcoite chondrules differ from the chondrule-size impact-melt spherules found in some achondritic breccias (e.g., Kapoeta; Brownlee and Rajan, 1973) and lunar rocks (e.g., Keil et al., 1972; Kurat et al., 1972; Symes et al., 1998; Ruzicka et al., 2000); the textural types of the chondrule-like objects in achondrites and lunar rocks are more restricted than those in chondritic meteorites or acapulcoites. (2) Acapulcoites contain planetary-type noble gases at higher concentrations than in equilibrated OC (e.g., Palme et al., 1981). Such gases are found in chondrites (e.g., Signer and Suess, 1963) and are absent from the differentiated HED meteorites (Hintenberger et al., 1969; Bogard et al., 1971; Begemann et al., 1976). Wasson (1985) stated that the presence of significant amounts of planetary gases in a meteorite is *prima facie* evidence that the sample was produced by "minor alteration of chondritic material rather than by igneous differentiation." (3) Acapulcoites have basic chondritic mineralogy (e.g., Table 5). They contain major olivine, low-Ca pyroxene, plagioclase and metallic Fe-Ni, minor Ca pyroxene and troilite, and accessory chromite and phosphate. The

Table 5  
Modal mineralogy (vol %) of the Monument Draw acapulcoite and H-group ordinary chondrites

|                 | Monument Draw | H chondrites |
|-----------------|---------------|--------------|
| Olivine         | 23.3          | 38           |
| Low-Ca pyroxene | 38.6          | 28           |
| Ca pyroxene     | 3.0           | 6            |
| Plagioclase     | 9.8           | 10           |
| Chromite        | Trace         | <1           |
| Phosphate       | 0.8           | <1           |
| Metallic Fe-Ni  | 13.9          | 10           |
| Troilite        | 5.6           | 5            |
| Limonite        | 4.9           | —            |
| Total           | 99.9          | $\geq 97$    |

Monument Draw data from McCoy et al. (1996); H-chondrite data from Table 5.1 of Hutchison (2004).

composition of plagioclase in the acapulcoites (e.g., Ab82Or4 in Acapulco; Ab81Or4 in ALH A77081 and ALH A81261; Palme et al., 1981; Schultz et al., 1982; Mittlefehldt et al., 1996) is slightly less potassic than (but otherwise similar to) that in OC (e.g., Ab82Or6 in mean H chondrites; Van Schmus and Ribbe, 1968). (4) The bulk compositions of acapulcoites are very similar to those of chondrites. For example, the CI- and Mg-normalized refractory lithophile abundances in Acapulco and ALH A77081 are close to unity (e.g., Palme et al., 1981; Kallemeyn and Wasson, 1985; Zipfel et al., 1995). Refractory siderophile elements also have CI-level abundances.

Among the chondrite groups, it is only the carbonaceous chondrites that have refractory lithophile abundances greater than or equal to CI; ordinary and enstatite chondrites have lower abundances (e.g., Fig. 1 of Wasson and Kallemeyn, 1988). Besides CI chondrites themselves (which lack chondrules), the only major group of carbonaceous chondrites that has CI-level abundances of refractory lithophiles and refractory siderophiles is the CR group (Kallemeyn et al., 1994).

The mean modal metallic Fe-Ni abundance in the acapulcoites ( $17 \pm 10$  wt%; Table 2) indicates that their precursor chondrites were probably metal rich. The carbonaceous chondrite group that includes the most metal-rich members is the CR group. Weisberg et al. (1993) reported that the CR chondrites Renazzo and Y 793495 contain 7.4 vol % (i.e.,  $\sim 16$  wt%) and 7.7 vol % (i.e.,  $\sim 17$  wt%) metallic Fe-Ni, respectively. If acapulcoites lost some metal during heating, their precursors must have been somewhat richer in metal than normal CR chondrites.

The mean apparent diameter of CR chondrules is 700  $\mu\text{m}$  (Table 2 of Rubin, 2000); the discernable relict chondrules in Dhofar 1222 also average  $\sim 700$   $\mu\text{m}$ .

In addition, acapulcoites resemble CR chondrites in O-isotopic composition. Acapulcoites and lodranites overlap in their ranges of  $\Delta^{17}\text{O}$  (i.e.,  $-0.85$  to  $-1.22\%$  and  $-0.85$  to  $-1.49\%$ , respectively; Clayton and Mayeda, 1996). The combined  $\Delta^{17}\text{O}$  range of acapulcoites and lodranites ( $-0.85$  to  $-1.49\%$ ) overlaps that of CR chondrites ( $-0.96$  to  $-2.42\%$ ; Clayton and Mayeda, 1999).

The cosmic-ray exposure (CRE) ages of acapulcoites (5–8 Ma; McCoy et al., 1996) resemble that of one CR chondrite (5.2 Ma for GRA 95229; Scherer and Schultz, 2000) but are much lower than that of Renazzo ( $\sim 22$  Ma) or Al Rais ( $\sim 44$  Ma) (ages calculated from the noble-gas data in Schultz and Kruse, 1989 using the production rates of Eugster, 1988).

The paucity of sulfide in CR chondrites ( $1.7 \pm 1.0$  vol %; Weisberg et al., 1993) compared to acapulcoites ( $6.0 \pm 4.3$  vol %; Table 2) makes normal CR chondrites unlikely precursors. McCoy et al. (1996) examined the possibility that CR chondrites and the ungrouped Kakangari chondrite are related to acapulcoites. They concluded that no firm relationship existed. I postulate here that acapulcoites formed from heretofore-undiscovered CR-like carbonaceous chondrites that were rich in sulfide and somewhat richer in metallic Fe-Ni than normal CR chondrites. It is not overly speculative to suggest that such groups might exist; there are numerous examples of ungrouped

carbonaceous chondrites (Grady, 2000; Huber et al., 2006), including ungrouped CR-like chondrites (e.g., GRO 95577; Weisberg and Prinz, 2000).

#### 4.2. Petrogenetic history of acapulcoites and lodranites

The petrogenesis of acapulcoites includes agglomeration of the precursor chondritic material (i.e., plausibly CR-like chondrites), heating of this material (inferred below to have been via collisions on the parent body), reduction at elevated temperatures, rapid cooling, moderate annealing, and in some cases, post-annealing shock.

Lodranites probably formed on the same parent body as acapulcoites (e.g., McCoy et al., 1997a,b; Mittlefehldt et al., 1996); this conclusion is consistent with the similarities between these groups in O-isotopic composition (Clayton and Mayeda, 1996) and is supported by their similarities in cosmic-ray-exposure ages (i.e., 4–7 Ma; Eugster and Lorenzetti, 2005). The principal difference in the petrogenetic histories of these two groups may be that lodranites experienced greater degrees of heating accompanied by loss of plagioclase and, in many cases, loss of a S-rich metallic melt.

##### 4.2.1. Heating

Benedix and Lauretta (2006) determined two-pyroxene temperatures for three acapulcoites: 950 °C for the primitive, relict-chondrule-bearing sample GRA 98028, and 1130 °C for relict-chondrule-free Acapulco and MET 01195. The latter temperature is appreciably above the Fe–FeS eutectic (988 °C; Brandes and Brook, 1998).

As pointed out by McCoy et al. (1996), acapulcoites are characterized by recrystallized textures consisting of equigranular silicates. Many grain boundaries converge at 120° triple junctures, indicating a high degree of textural equilibrium (e.g., Fig. 10).

Grain sizes in OC tend to increase with increasing recrystallization. For example, metallic Fe–Ni grains in H3 Sharps average ~65 μm (Benoit et al., 1998) whereas those in H5 and H6 chondrites average 120 μm (Table 2 of Rubin et al., 2001). As shown above, the average metal grain sizes in typical acapulcoites are ~200 μm in size; those in the acapulcoites Dhofar 1222 and LEW 86220 (the latter of which appears to be intermediate between acapulcoites and lodranites; McCoy et al., 1997b) average ~400 μm.

Indicators of heating in acapulcoites include the presence of metal and sulfide veins (Fig. 5), irregular troilite grains within metallic Fe–Ni (Fig. 7), fine-grained metal–troilite intergrowths (Fig. 6) and metallic Cu within metallic Fe–Ni grains (Fig. 8). All of these features resulted from localized melting of non-silicate phases. The mobilized occurrences of metal and sulfide indicate that local temperatures must have reached or exceeded the Fe–FeS eutectic temperature, i.e., 988 °C (Brandes and Brook, 1998). [At high impact-induced pressures, the Fe–FeS eutectic temperature increases (reaching 1202 °C at 25 GPa, i.e., 250 kb) and the proportion of S in the eutectic composition decreases (reaching 15.5 wt% S at 24 GPa) (Fei et al., 2006).]

Metallic Cu grains within metallic Fe–Ni form after localized melting of metal–troilite assemblages at temperatures near or above the eutectic. Melting is followed by

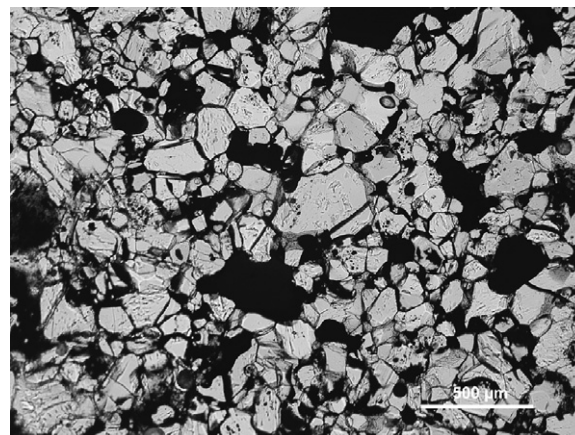


Fig. 10. Recrystallized texture of acapulcoite ALH A77081 showing that many silicate grains meet each other at 120° triple junctures. This indicates a high degree of textural equilibrium. Clear phases are silicates; black regions are opaques (metallic Fe–Ni and troilite). Transmitted light.

crystallization of taenite, supersaturation of Cu in the residual sulfide-rich melt, and nucleation of small patches of metallic Cu at high-surface-energy sites, typically along metal–sulfide grain boundaries (Rubin, 1994). The taenite crystal structure can accommodate ~16 times more Cu than that of kamacite (Hansen, 1958); when kamacite forms at the expense of taenite during cooling of the metallic Fe–Ni assemblage below the Fe–Ni solvus, metallic Cu precipitates as a separate phase.

CR chondrites contain ~54 vol % chondrules and chondrule fragments (Weisberg et al., 1993). The acapulcoite with the greatest modal abundance of recognizable relict chondrules is GRA 98028 (with ~6 vol %) (e.g., Fig. 1a). Most acapulcoites contain no recognizable relict chondrules. If acapulcoites formed from CR-like chondrites, then some process must have obliterated ~90–100% of the chondrules in the precursors. The low abundance of recognizable chondrules in highly recrystallized type-6 OC (e.g., LL6 Manbroom and L6 Putinga; Mason and Wiik, 1964; Gomes and Keil, 1980) and in OC impact-melt rocks (e.g., “L7” PAT 91501; Mittlefehldt and Lindstrom, 2001) suggests that the dearth of chondrules in acapulcoites is due to appreciable heating involving either extensive solid-state recrystallization or minor-to-moderate degrees of melting. In metamorphosed OC, small chondrules are preferentially integrated with the matrix, leading to an increase in the average size of surviving chondrules (e.g., Hutchison, 2004); however, the average apparent diameter of relict chondrules in the Dhofar 1222 acapulcoite is 700 μm, identical to those in the presumptive CR-like chondrite precursor (Table 2 of Rubin, 2000). The complete absence of relict chondrules in most acapulcoites seems more consistent with minor-to-moderate melting. Acapulcoites thus may have been heated to ~1100 °C (the approximate OC solidus temperature; Jurewicz et al., 1995). Nevertheless, the absence of igneous textures in these rocks indicates that melting was not extensive.

Compared to acapulcoites, lodranites have coarser silicate grains (e.g., Fig. 8.3a,b of Hutchison, 2004) and

coarser metal grains (e.g., metal in the EET 84302 lodranite has a mean size of  $\sim 1000 \mu\text{m}$ ). Most lodranites are depleted in plagioclase and troilite relative to acapulcoites, suggesting that lodranites were more significantly heated and suffered partial melting (Mittlefehldt et al., 1996; McCoy et al., 1997a,b; Floss, 2000). The absence of relict chondrules in lodranites is consistent with the formation of lodranites at higher temperatures than acapulcoites. McCoy et al. (1997a) estimated that lodranites reached temperatures of  $\sim 1050\text{--}1200 \text{ }^\circ\text{C}$ ; at the latter temperature, chondritic matter should be  $\sim 20\%$  molten (depending on composition) and (depending on the size and structure of the asteroid) capable of gravitational separation of metallic and basaltic (plagioclase- and pyroxene-rich) liquids.

El Goresy et al. (2005) proposed that those silicate grains in acapulcoites and lodranites that contain ovoid clusters of small metal and troilite blebs in their centers (e.g., Fig. 10) formed by decoration of the boundaries of residual silicate grains during partial melting. I suggest an alternative: the clusters of opaque grains within silicate centers may have resulted from relict opaque-bearing silicate grains being overgrown by inclusion-free silicate crystallizing from the impact melt. The relict opaques may have formed from shocked silicate grains exhibiting “darkening” as a result of molten opaques having been shock-injected into silicate fractures (e.g., Rubin, 1992). The lower  $\text{TiO}_2$  and  $\text{Al}_2\text{O}_3$  in the small chromite grains within the opaque clusters (Table 3) indicates that they formed or equilibrated at lower temperatures (e.g., Fig. 4 of Sack and Ghiorso, 1991) than the coarser chromite grains in the matrix. If the opaque clusters were once fine-grained, shock-injected grains, it seems plausible that subsequent annealing (see below) could have caused coarsening of the silicates and the opaque blebs inside them.

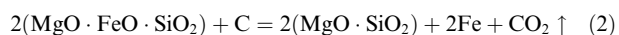
#### 4.2.2. Reduction

Reduction was probably responsible for producing several of the principal petrographic and mineralogical characteristics of acapulcoites and lodranites. The presence of graphite in some of these rocks (e.g., MET 01195 and GRA 95209; e.g., Fig. 4) indicates that carbon was probably the reducing agent. As discussed above, CR-like carbonaceous chondrites may have been the precursors of acapulcoites. CR chondrites contain  $\sim 1.4 \text{ wt}\% \text{ C}$  (Mason and Wiik, 1962), probably present mainly as organic matter in the matrix. Although Ramdohr (1973) listed graphite as a constituent of CR2 Renazzo, other workers (e.g., Bischoff et al., 1993; Weisberg et al., 1993) have not reported graphite in any CR chondrite.

Reduction most likely took place at elevated temperatures via a reaction similar to one of the following:



or



These reactions produce metallic Fe at the expense of FeO, resulting in minor increases in the metal abundances and metal/troilite ratios of acapulcoites. The reactions might

also cause enhancements in the bulk Fe/Ni ratios of the metal as reflected by the kamacite/taenite ratios in acapulcoites. In addition, if acapulcoites lost some metallic Fe–Ni after being heated above the Fe–Ni–S eutectic temperature, the lost metallic melt would have been rich in Ni and S (Kullerud, 1963), accounting in part for the residual high metal/troilite ratios in many acapulcoites.

Benedix and Lauretta (2006) calculated an oxygen fugacity for acapulcoites of  $\sim 2.3$  log units below the iron-wüstite (IW) buffer. This is similar to that of equilibrated H chondrites, i.e., 2.10 to 2.56 log units below the IW buffer (Kessel et al., 2004), although these values are appreciably lower than that of OC determined earlier by Brett and Sato (1984), i.e., 0.4 to 1.1 log units below IW.

Crystallization of mafic silicates from reduced melts (i.e., liquids with relatively low FeO) may have produced the reverse zoning observed in mafic grains in some acapulcoites and lodranites. For example, Yugami et al. (1993) reported significant reversed zoning in orthopyroxene (opx) grains in the acapulcoite ALH A81187 and in the lodranite Y 74357. The *mg* numbers  $[(\text{Mg} \times 100)/(\text{Fe} + \text{Mg})]$  of ALH A81187 opx vary from 94 in the core to 98 in the rim; those in Y 74357 opx vary from 86 in the core to 92 in the rim. In contrast, Acapulco and Monument Draw show no zoning in FeO or MgO in their mafic silicate grains (Zipfel et al., 1995; McCoy et al., 1996). The absence of compositional zoning in these rocks could possibly be due to enhanced Fe–Mg diffusion causing flattening of zoning profiles during annealing.

Bild and Wasson (1976) reported reverse zoning in olivine grains (but not pyroxene grains) in Lodran. McCoy et al. (1997a) reported reverse zoning in pyroxene grains in several lodranites (i.e., Gibson, FRO 90011, Y 74357 and Y 791493).

The amount of FeO available for incorporation into olivine and low-Ca pyroxene decreases with increasing reduction, resulting in lower mean Fa and Fs values than in the original precursor rock. Because diffusion of Mg and Fe in olivine is more rapid than in pyroxene (Buening and Buseck, 1973; Freer, 1981; Chakraborty, 1997), olivine in a reduced rock will tend to equilibrate faster and achieve a higher *mg* number than low-Ca pyroxene. Thus, comparisons of acapulcoites with equilibrated chondrites is a worthwhile exercise. Among equilibrated OC, mean olivine Fa values exceed mean opx Fs values. The difference between Fa and Fs is a function of composition: among LL chondrites, mean Fa is 4.4 mol% higher than mean Fs (28.5 vs. 24.1); among L chondrites, Fa is 3.3 mol% higher (24.6 vs. 21.3); and among H chondrites, Fa is 1.6 mol% higher (18.8 vs. 17.2) (Gomes and Keil, 1980). With increasingly reduced compositions, the difference between Fa and Fs values decreases. For the 38 probably unpaired acapulcoites and lodranites for which both olivine and low-Ca pyroxene data are available (Table 6), 26 (68%) have  $\text{Fa} \leq \text{Fs}$ . However, the values are not systematic: some acapulcoites have  $\text{Fa} < \text{Fs}$  (e.g., 12.7 vs. 13.0 mol% in NWA 3008); others with similar Fa values have  $\text{Fa} > \text{Fs}$  (e.g., 13.1 vs. 12.2 mol% in NWA 2627). The same non-systematic behavior occurs in more reduced samples: e.g., 4.6 mol% Fa vs. 6.9 mol% Fs in Superior Valley 014, and

Table 6  
Olivine and low-Ca pyroxene compositions

| Meteorite               | Fa (mol%) | Fs (mol%) |
|-------------------------|-----------|-----------|
| <i>Acapulcoites</i>     |           |           |
| Acapulco                | 11.9      | 12.6      |
| ALH A77081              | 10.7      | 10.5      |
| ALH A81187              | 4.2       | 3.3       |
| Dhofar 125              | 8.5       | 7.7       |
| Dhofar 290              | 11        | 10.5      |
| Dhofar 312              | 8.6       | 7.6       |
| Dhofar 1222             | 6.8       | 8.1       |
| FRO 95029               | 8.3       | 8.5       |
| GRA 98028               | 8–9       | 8–10      |
| LAP 031323              | 13        | 12        |
| LEW 86220               | 7         | 9         |
| MAC 041193 <sup>a</sup> | 11        | 11        |
| MET 01195               | 8–9       | 9         |
| Monument Draw           | 10.1      | 10.6      |
| NWA 1052                | 6.0       | 7.6       |
| NWA 2627                | 13.1      | 12.2      |
| NWA 2656                | 8.0       | 8.4       |
| NWA 2775                | 14.5      | 13.3      |
| NWA 3008                | 12.7      | 13.0      |
| RBT 04228               | 8         | 10        |
| Superior Valley 014     | 4.6       | 6.9       |
| TIL 99002               | 9.2       | 9–11      |
| Y 74063                 | 10.9      | 10.9      |
| Y 8307                  | 10.3      | 9.8       |
| <i>Lodranites</i>       |           |           |
| EET 84302               | 8.1       | 8.1       |
| FRO 90011               | 9.4       | 12.6      |
| FRO 93001               | 13.3      | 13.3      |
| FRO 99030               | 10        | 12        |
| FRO 03001               | 9.5       | 13.2      |
| Gibson                  | 3.1       | 5.8       |
| GRA 95209               | 7         | 7         |
| LEW 88280               | 13        | 11.9      |
| Lodran                  | 13.2      | 12.6      |
| MAC 88177               | 13.7      | 12.8      |
| NWA 2235                | 12        | 13        |
| Y 74357                 | 7.9       | 13.8      |
| Y 75274                 | 3.9       | 3.9       |
| Y 791491                | 10.7      | 11.7      |

Literature data from McCoy et al. (1996, 1997a), Mittlefehldt et al. (1996), Yanai (2001), and several editions of *The Meteoritical Bulletin* and *Antarctic Meteorite Newsletter*. Probably paired samples are excluded from the table.

<sup>a</sup> MAC 041193 is listed in *Ant. Met. Newslett.* 29, 2 as transitional between acapulcoites and lodranites.

4.2 mol% Fa vs. 3.3 mol% Fs in ALH A81187. The appreciably lower Fa values in some acapulcoites and lodranites relative to their Fs values (Table 6) are indicative of substantial reduction.

Loss of FeO causes a decrease in the FeO/MnO ratio in olivine (e.g., Fig. 3a of Mittlefehldt, 1990); FeO is more readily reduced than MnO in part because the iron-oxygen bond is weaker than the manganese-oxygen bond. One consequence of this is that the MnO concentration is not lower in olivine from the more-reduced equilibrated OC: Table A3.34 of Brearley and Jones (1998) shows a mean MnO content in olivine in equilibrated H chondrites (which have

the lowest Fa among the three main OC groups) of 0.51 wt%; that in L and LL chondrite olivine is 0.50 and 0.43 wt%, respectively. Equilibrated H chondrites have olivine FeO/MnO ratios in the range of 32–38 (Table A3.34 of Brearley and Jones, 1998); in contrast, acapulcoite olivines have ratios of 16–18 (Table 2 of McCoy et al., 1996), and lodranite olivines have ratios of 8–25 (Table 3 of McCoy et al., 1997a). These low FeO/MnO ratios are indicative of reduction.

Another consequence of reduction is an increase in the opx/olivine ratio (e.g., McSween and Labotka, 1993) as shown in reactions 1 and 2 above. Although H chondrites have modal opx/olivine ratios of ~0.74 (Table 5.1 of Hutchison, 2004), some acapulcoites have much higher opx/olivine modal ratios: Monument Draw, 1.7 (McCoy et al., 1996); Dhofar 312, 1.4 (Grossman and Zipfel, 2001); and NWA 2627, 1.1 (Russell et al., 2005). In contrast, the lodranite Y 791491 is unusual in having a modal opx/olivine ratio of 0.7 (Kojima and Imae, 1998), similar to that of H chondrites.

An alternative explanation for the relatively high opx/olivine ratios in acapulcoites is that these rocks formed from an already reduced assemblage (D.W. Mittlefehldt, pers. commun., 2006). However, in view of the significant evidence for reduction in acapulcoites, it seems plausible that their high opx/olivine ratios are largely the result of active reduction occurring at high temperatures.

Finally, with increasing degrees of reduction, some phosphate could have been transformed into phosphide. Although phosphide is uncommon in ordinary and carbonaceous chondrites, schreibersite [(Fe,Ni)<sub>3</sub>P] was reported in the Dhofar 1222 acapulcoite (Russell et al., 2005) and in the FRO 99030 lodranite (Grossman, 2000). Moggi-Cecchi et al. (2005) reported a new Ni-Fe phosphide [(Ni,Fe)<sub>4</sub>P] as being a “rather common” phase in the probably paired acapulcoites NWA 1052 and 1054.

The relatively large variations in the properties of different acapulcoites and lodranites indicate that different rocks experienced different degrees of alteration. These variations are apparent in (a) the mean olivine and low-Ca pyroxene compositions (Fa 4.2–14.5 and Fs 3.3–13.3 in acapulcoites; Fa 3.1–13.7 and Fs 3.7–13.8 in lodranites), (b) the olivine FeO/MnO ratios (16–18 in acapulcoites; 8–25 in lodranites), and (c) the modal opx/olivine ratios (1.1–1.7 in acapulcoites, but only 0.7 in one lodranite).

#### 4.2.3. Cooling history

In a study of (U–Th)/He ages of phosphate grains in Acapulco, Min et al. (2003) deduced that this meteorite cooled slowly (on the order of 25 °C/Ma) through the temperature range of ~550–120 °C. This rate is basically consistent with those deduced by Zipfel et al. (1995) and Pellas et al. (1997) from inferred maximum temperatures, the Pb–Pb age of phosphate grains, and <sup>244</sup>Pu and <sup>40</sup>Ar–<sup>39</sup>Ar chronometers, i.e., ~100 °C/Ma between 1100 ± 100 °C and 500 ± 50 °C. Pellas et al. inferred even slower cooling at lower temperatures: ~1–4 °C/Ma below 450 °C. These rates are irreconcilable with those measured by Zipfel et al. (1995) for Ca in acapulcoite olivine: 800–1000 °C/Ma. Much slower cooling rates were reported by

Zema et al. (1996); these workers measured Fe<sup>2+</sup>-Mg ordering in orthopyroxene in Acapulco and ALH 81261 (paired with ALH A77081) and determined cooling rates of ~0.17 °C/day at 490 °C and ~0.05 °C/day at 465 °C, respectively. These large discrepancies in cooling rates point to a complicated thermal history for the acapulcoites and lodranites. Slow cooling could indicate either deep burial within an internally heated body (e.g. Zipfel et al., 1995) or burial beneath an ejecta blanket or fallback material of low thermal diffusivity at an impact site. More rapid cooling is consistent with impact heating and shallow burial.

Molin et al. (1994) inferred a cooling rate of ~3 °C/day at 530 °C for the FRO 90011 lodranite from separated orthopyroxene grains analyzed by X-ray diffraction, electron microprobe and TEM techniques.

Some acapulcoites display a lack of large-scale textural equilibrium; they are heterogeneous on scales of several millimeters. LEW 86220 has regions with coarse metal that resemble the texture of a lodranite and regions with finer-grained metal typical of acapulcoites (McCoy et al., 1997b). As pointed out by El Goresy et al. (2005), such features are not commonly observed in unbrecciated type-6 OC. Lack of equilibrium is also shown by the distinct populations of chromite in Acapulco that exhibit different chemical zoning trends (El Goresy et al., 2005). Because diffusion in chromite is appreciably more rapid than in olivine (e.g., Wilson, 1982), such textural and mineralogical disequilibrium in acapulcoite chromite is consistent with rapid cooling.

The relatively high concentrations of planetary-type noble gases in acapulcoites (e.g., Palme et al., 1981) are consistent with rapid cooling. Slow cooling from elevated temperatures is likely to lead to loss of such gases as apparently occurred in the HED meteorites (e.g., Hintenberger et al., 1969; Bogard et al., 1971; Begemann et al., 1976). Planetary-type noble gases are characteristic of chondrites (e.g., Signer and Suess, 1963), including OC impact-melt breccias (e.g., Belle Plaine, Madrid, Orvinio, Rose City, Shaw, Taiban) (e.g., Schultz and Kruse, 1989).

#### 4.2.4. Nature of heating mechanism

Many of the petrographic features in acapulcoites could have been produced by shock heating. Although not itself a shock indicator, the occurrence of rare relict chondrules in some of these rocks demonstrates appreciable heating. The textures of the relict-chondrule-bearing acapulcoites are analogous to those of the relict-chondrule-bearing regions of the L-chondrite impact-melt rock PAT 91501 (Mittlefehldt and Lindstrom, 2001), the H-chondrite impact-melt breccias Spade (Rubin and Jones, 2003) and LAP 02240 (e.g., Swindle et al., 2006), and the EH-chondrite impact-melt breccia Abee (Rubin and Keil, 1983; Rubin and Scott, 1997). They are also analogous to the textures of many silicate clasts in the H-chondrite impact-melt-breccia Portales Valley (which have a paucity of chondrules) (Rubin et al., 2001) and to the matrix of the EH-chondrite impact-melt breccia Adhi Kot (Rubin, 1983; Rubin and Scott, 1997). The phenocrysts within relict chondrules in GRA 98028 that contain curvilinear trails of small blebs of metallic Fe-Ni and troilite exhibit “silicate darkening” (Rubin,

1992); these relict chondrules thus constitute examples of shocked but unmelted precursor material.

Fine-grained metal-sulfide intergrowths are prevalent in chondrites of shock stages S3-S6 and have been interpreted as having formed by impact heating and quenching (Scott, 1982). Although such assemblages could form near the fusion crust of a meteorite during atmospheric passage, their occurrence in the interior of a chondrite is considered to be a reliable shock indicator (Scott, 1982).

Metal and sulfide veins commonly occur in shocked chondrites (e.g., Smith and Goldstein, 1977; Stöffler et al., 1991; Bennett and McSween, 1996a). These veins traverse shocked mafic silicate grains (e.g., Fig. 18 of Stöffler et al., 1991) and fractured chromite grains (e.g., Fig. 1c,d of Rubin, 2003) in moderately (shock-stage S4) to very strongly shocked (shock-stage S6) chondrites. Some metal veins in acapulcoites traverse mafic silicate grains (e.g., Fig. 5a); other veins follow silicate grain boundaries. In the latter case, it seems possible that annealing caused distinct silicate grains to form on either side of a metal vein that originally cut through a single silicate grain.

Shock is also responsible for forming polycrystalline kamacite in acapulcoites. This feature has been observed in many shocked chondrites (e.g., Taylor and Heymann, 1971; Bennett and McSween, 1996a) and is indicative of shock stage S4-S5 (Schmitt et al., 1993). Low-Ni taenite can transform into polycrystalline kamacite during quenching (e.g., Speich and Swann, 1965). The coarse grain sizes of these polycrystalline assemblages in acapulcoites may reflect moderate post-shock annealing.

Irregularly shaped troilite grains within metallic Fe-Ni occur within many shock-stage S3-S6 OC (e.g., Fig. 2c of Rubin, 1994). These assemblages are inferred to have formed by disequilibrium minor melting of metal-sulfide assemblages followed by rapid cooling. Their occurrence in numerous shocked OC suggests that they are a reliable shock indicator, although at present there is no experimental evidence for the formation of these textures.

Metallic Cu grains occur within metallic Fe-Ni in shocked meteorites. In some shocked OC, metallic Cu rinds occur around metallic Fe-Ni dendrites in rapidly solidified metal-troilite assemblages (Fig. 2a of Rubin, 1994); in other cases, metallic Cu occurs at the interface between metal and sulfide in opaque shock veins (Fig. 2b of Rubin, 1994). In these cases, the inversion of taenite to kamacite corresponds to a significant decrease in the solubility of Cu in the metallic Fe-Ni; exsolution of the metallic Cu occurs at the metal-sulfide interfaces. These petrographic associations with shock features make it likely that the presence of metallic Cu is not due to long-period heating during thermal metamorphism. If that were the case, type-6 OC would contain appreciably more metallic Cu than OC of lower petrologic types; they do not (Rubin, 1994).

Although the proportion of metallic-Cu-bearing OC is independent of shock stage (Rubin, 1994), this does not mean that El Goresy (2006) is correct in suggesting that metallic Cu is not a valid shock indicator. Many OC could have been shocked and annealed, a process leading to erroneously low apparent shock stages (Rubin, 2004). Thus, a

shock-stage S1 or S2 OC could have had a maximum prior shock stage that was appreciably higher before annealing.

The common occurrence in shocked OC of rapidly solidified metal–troilite assemblages, metal and sulfide veins, irregularly shaped troilite grains within metallic Fe–Ni grains, and metallic Cu within metallic Fe–Ni strongly suggest that all of these features are reliable shock indicators (Rubin, 2004). There are correlations among these features: among those type-5-6 OC of shock stage S1–S2 that contain metal–sulfide veins, ~50% also contain rapidly solidified metal–troilite assemblages, and ~50% also contain irregular grains of troilite within metallic Fe–Ni (Rubin, 2004). There are also correlations among these features in the acapulcoites: GRA 98028 contains metal veins and irregular grains of troilite in metal; LEW 86220 contains metal veins, sulfide veins, and irregular grains of troilite in metal; ALH 84190 contains troilite veins, polycrystalline kamacite, and rapidly solidified metal–sulfide assemblages; and ALH A77081 contains troilite veins and rapidly solidified metal–sulfide assemblages.

The presence of phosphide in some acapulcoites and lodranites (Dhofar 1222, NWA 1052 and 1054, FRO 99030; Grossman, 2000; Moggi-Cecchi et al., 2005; Russell et al., 2005) may also be evidence of shock. Although phosphide is very rare in unshocked OC, it does occur in several highly shocked OC (Ramsdorf, Orvinio, Rose City, Farmington, Lubbock; Smith and Goldstein, 1977) and within an impact-melt-rock clast in the Dimmitt H-chondrite regolith breccia (Rubin et al., 1983). Phosphide apparently formed in these samples by the melting of P-bearing metal (or metal-phosphate assemblages; Rubin and Grossman, 1985) and the precipitation of phosphide grains at metal–sulfide boundaries.

The occurrence of these shock features in several acapulcoites suggests that the acapulcoites were heated by impacts, as first suggested by Kallemeyn and Wasson (1985). Moderate degrees of melting associated with impact-heating destroyed most of the chondrules.

Also consistent with a shock origin for acapulcoites is the diversity of young He ages for phosphate grains in Acapulco; Min et al. (2003) concluded that these age variations are probably due to “heterogeneous heating caused by collision event(s).”

Lodranites experienced more heating than acapulcoites. Their low amounts of plagioclase may indicate partial melting and loss of a basaltic (plagioclase–pyroxene) partial melt (McCoy et al., 1997b). The low plagioclase abundances in lodranites reflects the greater degree of heating experienced by these rocks, a process resulting in a higher degree of plagioclase loss. The coarser grain size and absence of relict chondrules in lodranites are consistent with greater heating, slower cooling, and more extensive recrystallization of these rocks.

The low troilite abundances (0.1–3.8 wt%) and high metallic-Fe–Ni/troilite ratios (40–430) in many lodranites (Table 2; Fig. 2c) are consistent with loss of an Fe–Ni–S melt (Mittlefehldt et al., 1996). This inference is supported by the low bulk Se in the EET 84302 lodranite and anti-correlations between Ir/Ni and Se/Co in acapulcoites and lodranites (Fig. 6 of Mittlefehldt et al., 1996). The LEW

86220 acapulcoite (which is texturally intermediate between acapulcoites and lodranites) has a moderately high metallic-Fe–Ni/troilite ratio (6.1) and also may have lost a S-rich melt. Such Fe–Ni–S melts may have intruded the lodranites LEW 88280 and MAC 88177 (Mittlefehldt et al., 1996), accounting for the relatively low metallic-Fe–Ni/troilite ratios in these rocks (4.8 and 0.6, respectively; Table 2). Because melting would have obliterated the shock features in MAC 88177, this shock-stage S5 rock must have been shocked again after cooling.

Mittlefehldt et al. (1996) concluded that acapulcoites and lodranites were heated on their parent body by processes that were “localized and heterogeneous in space and time.” This appears inconsistent with heating by the decay of <sup>26</sup>Al. This mechanism should cause global heating of the asteroid over millions of years (e.g., Bennett and McSween, 1996b; Keil, 2000) and produce large batches of uniformly heated material.

Immediately after the impact event(s), the acapulcoites and lodranites would have exhibited numerous shock effects including undulose extinction in olivine, metal and sulfide veins, metallic Cu, and irregularly shaped troilite grains in metallic Fe–Ni. It is also possible that low-Ca clinopyroxene would have been present; Hornemann and Müller (1971) and Stöffler et al. (1991) found that clinopyroxene lamellae parallel to (100) form within opx grains at shock pressures of ~5 GPa (i.e., 50 kb). The paucity of olivine grains with pronounced undulose extinction and the absence of low-Ca clinopyroxene in acapulcoites and lodranites may attest to post-shock annealing as discussed below.

#### 4.2.5. Post-shock annealing

McCoy et al. (1996) dismissed impacts as a viable mechanism for heating the acapulcoites because the olivine grains in these meteorites typically exhibit either sharp optical extinction (characteristic of shock-stage S1) or undulose extinction (characteristic of shock-stage S2). Nevertheless, post-shock annealing processes can heal damaged olivine crystal lattices (Bauer, 1979; Ashworth and Mallinson, 1985) and make the rocks appear less shocked than they were previously (Rubin, 2002, 2003; Rubin and Jones, 2003). For example, the olivine grains in LL6 MIL 99301 exhibit sharp optical extinction despite the occurrence of numerous curvilinear trails of small blebs of metal and sulfide (characteristic of shocked OC; Rubin, 1992) that were presumably injected into the olivine by shock processes (e.g., Fig. 4 of Rubin, 2002). If the olivine grains in MIL 99301 had been mosaiced by the initial shock event, then they would have formed polycrystalline aggregates of unstrained olivine crystals as has occurred in several ureilites (Rubin, 2006); the absence of polycrystallinity in MIL 99301 olivine grains indicates that the original olivine crystals were not mosaiced during shock.

Support for impact-induced heating comes from the <sup>39</sup>Ar–<sup>40</sup>Ar age of MIL 99301; this rock was annealed ~4.26 Ga ago (Dixon et al., 2004). At this late date, i.e., ~300 Ma after accretion, an impact event is the only plausible heat source; <sup>26</sup>Al would have long-since decayed away (more than 400 half-lives would have passed).

If any high-pressure phases (e.g., ringwoodite, majorite) had been formed in acapulcoites during initial shock, post-shock annealing after the release of pressure would have caused these phases to revert to their low-pressure polymorphs (i.e., olivine, orthopyroxene) (e.g., Chen et al., 1996).

Another potential shock feature that could have been erased in acapulcoites by annealing is the occurrence of low-Ca clinopyroxene (assuming that this phase had formed from orthopyroxene during an earlier shock event; Hornemann and Müller, 1971; Stöffler et al., 1991). Within certain compositional constraints, this phase transforms into orthopyroxene at  $\geq 630$  °C (Boyd and England, 1965; Grover, 1972).

One objection to impact heating is that many of the metal veins in acapulcoites occur in between silicate grains rather than transecting them as in shocked OC. However, as discussed above, during annealing, silicate grains transected by metal veins would tend to recrystallize and form individual grains separated by the metal veins.

On the other hand, many relict shock indicators are likely to survive annealing. These include metallic Cu, metallic Fe–Ni and sulfide veins, and irregularly shaped troilite grains within metallic Fe–Ni. Coarse polycrystalline kamacite is also likely to survive moderate annealing; finely polycrystalline kamacite may have coarsened during annealing.

The graphite occurrences in acapulcoites and lodranites exhibit a diversity of morphologies and structures (e.g., El Goresy et al., 1995, 2005). Extensive post-shock annealing would tend to produce fine-grained, well-ordered graphite. It would also tend to homogenize the diverse C- and N-isotopic compositions of the graphite occurrences (El Goresy et al., 2005). These observations indicate that, at least in those few acapulcoites and lodranites that contain heterogeneous graphite, post-shock annealing was limited. Nevertheless, El Goresy et al. (1995) inferred that the heterogeneous graphite occurrences in Acapulco could survive the thermal conditions they accepted for this rock: 20% partial melting at equilibration temperatures of  $\sim 1200$  °C (Zipfel et al., 1995).

I conclude that acapulcoites and lodranites were heated by impacts, buried beneath material of low thermal diffusivity, and moderately annealed. After annealing, the olivine in these rocks would have exhibited sharp optical extinction indicative of shock-stage S1. (It seems unlikely that annealing would be so precise as to allow planar fractures and planar deformation features in olivine to heal and still leave enough crystal damage for the grains to exhibit undulatory extinction characteristic of shock-stage S2.)

Rubin (2004) examined 53 shock-stage S1 OC of petrologic type 5 and 6 and reported chromite veinlets in 100%, chromite–plagioclase assemblages in 100%, metallic Cu in 28%, irregular troilite grains within metallic Fe–Ni in 62%, and metal–sulfide veins in 21% of the samples. (Other relict shock indicators were also identified in many of these rocks.) All of these OC appear to have been shocked and annealed.

Other meteorite groups that have many members that appear to have been shocked and annealed include CK chondrites (Rubin, 1992), ureilites (Rubin, 2006), and EL

chondrites (Rubin et al., 1997). [Nevertheless, extensive shock melting of EL3 chondrites more than  $\sim 15$  Ma after accretion is precluded by the presence of excess  $^{53}\text{Cr}$  in EL3 sphalerite (El Goresy et al., 1992); if such heating had occurred after this time, the isotopic anomaly would have been erased. If shock melting had instead occurred prior to appreciable decay of  $^{53}\text{Mn}$  ( $t_{1/2} = 3.7$  Ma), then excess  $^{53}\text{Cr}$  could still have been produced in the sphalerite.]

Although impact heating cannot be a global process (Keil et al., 1997; McSween et al., 2002), it seems plausible that annealing could occur in shocked rocks buried beneath an insulating regolith or megaregolith. It seems likely that the same impact event responsible for the shock features in these rocks buried them and provided the heat necessary for annealing.

Many asteroids appear to be high-porosity bodies akin to rubble piles with densities as low as  $1.2 \text{ g cm}^{-3}$  (Bottke et al., 1999; Cheng and Barnouin-Jha, 1999; Veverka et al., 1999). In porous asteroids, collisional kinetic energy is distributed through relatively small volumes of material (Stewart and Ahrens, 1999) and efficiently converted into heat in the crater vicinity (Melosh, 1989; Housen and Holsapple, 1999; Britt et al., 2002). A residual component of the kinetic energy of the projectile is converted into thermal energy after the shock wave dissipates. The thermal energy is released from non-adiabatic decay of the shock wave (Raikes and Ahrens, 1979) and can induce static metamorphism in adjacent materials.

It is to be expected that different meteorite groups experienced similar shock and annealing processes. If one 20- to 50-km porous body in the asteroid belt was pelted by large meteoroids and underwent localized shock and annealing, then other similarly located bodies of similar size and structure would probably have been likewise affected.

#### 4.2.6. Post-annealing shock

If annealing caused olivine grains to heal their damaged crystal lattices and develop sharp optical extinction, then those acapulcoites and lodranites that are currently shock-stage S2 or higher must have been shocked again after annealing. Among the set of samples in this study, this would include the acapulcoites ALH 84190 (S3), Dhofar 1222 (S2), LEW 86220 (S2) and Superior Valley 014 (S2), and the lodranite MAC 88177 (S5).

Many equilibrated OC (Rubin, 2004) and some ureilites (Rubin, 2006) are also inferred to have experienced post-annealing shock. It seems likely that repeated impact events caused some rocks to undergo multiple episodes of shock and annealing (e.g., Lambert et al., 1984; Rubin, 2004).

## 5. CONCLUSIONS

Acapulcoites and lodranites formed by shock melting of CR-like precursor materials; lodranites were more extensively heated than acapulcoites. Acapulcoites exhibit numerous shock effects including veins of metallic Fe–Ni and troilite, polycrystalline kamacite, rapidly solidified metal–troilite assemblages, metallic Cu, and irregularly shaped troilite grains within metallic Fe–Ni. A few acapulcoites preserve a few volume-percent relict chondrules. While at

elevated temperatures, acapulcoites experienced extensive reduction that produced low olivine Fa and low-Ca pyroxene Fs contents, low FeO/MnO ratios in olivine, relatively high orthopyroxene/olivine ratios, and reverse zoning in some mafic silicate grains.

Rapid cooling allowed the retention of relatively high concentrations of planetary-type noble gases. Acapulcoites and lodranites were buried beneath an insulating, comminuted regolith (produced, at least in part, during the same impact events that shocked these meteorite groups) and underwent moderate post-shock annealing. This allowed the damaged olivine crystal lattices to be repaired, making the rocks appear unshocked. A few acapulcoites and lodranites experienced post-annealing shock and reached higher shock stages (e.g., S5 in the case of lodranite MAC 88177).

#### ACKNOWLEDGMENTS

I thank the Antarctic Meteorite Working Group for the loan of many of the thin sections. I am grateful to L. Labenne for his help in procuring pieces of Dhofar 1222. I am also grateful to K. Ziegler for determining the O-isotopic composition of Superior Valley 014. I thank J. T. Wasson, T. J. McCoy and D. W. Mittlefehldt for their comments on this study. This manuscript benefited from detailed reviews by A. Ruzicka, A. El Goresy, J. Zipfel and an anonymous reviewer. I also thank Associate Editor A. N. Krot for his comments and his patience. This work was supported by NASA Grant No. NNG06GF95G.

#### REFERENCES

- Ashworth J. R., and Mallinson L. G. (1985) Transmission electron microscopy of L-group chondrites, 2. Experimentally annealed Kyushu. *Earth Planet. Sci. Lett.* **73**, 33–40.
- Bauer J. F. (1979) Experimental shock metamorphism of mono- and polycrystalline olivine: a comparative study. *Proc. Lunar Planet. Sci. Conf.* **10**, 2573–2596.
- Begemann F., Weber H. W., Vilcsek E., and Hintenberger H. (1976) Rare gases and  $^{36}\text{Cl}$  in stony-iron meteorites: cosmogenic elemental production rates, exposure ages, diffusion losses and thermal histories. *Geochim. Cosmochim. Acta* **40**, 353–368.
- Benedix G. K., and Lauretta D. S. (2006) Thermodynamic constraints on the formation history of acapulcoites. *Lunar Planet. Sci.* **37**. Lunar Planet. Inst., Houston. #2129 (abstr.).
- Bennett M. E., and McSween H. Y. (1996a) Shock features in iron-nickel and troilite of L-group ordinary chondrites. *Meteorit. Planet. Sci.* **31**, 255–264.
- Bennett M. E., and McSween H. Y. (1996b) Revised model calculations for the thermal histories of ordinary chondrite parent bodies. *Meteorit. Planet. Sci.* **31**, 783–792.
- Benoit P. H., Akridge G., and Sears D. W. G. (1998) Size sorting of metal, sulfide, and chondrules in Sharps (H3.4) (abstract). *Lunar Planet. Sci.* **29**. #1457 (abstr.).
- Bild R. W., and Wasson J. T. (1976) The Lodran meteorite and its relationship to the ureilites. *Mineral. Mag.* **40**, 721–735.
- Bischoff A., Palme H., Ash R. D., Clayton R. N., Schultz L., Herpers U., Stöffler D., Grady M. M., Pillinger C. T., Spettel B., Weber H., Grund T., Endreß M., and Weber D. (1993) Paired Renazzo-type (CR) carbonaceous chondrites from the Sahara. *Geochim. Cosmochim. Acta* **57**, 1587–1603.
- Bogard D. D., Huneke J. C., Burnett D. S., and Wasserburg G. J. (1971) Xe and Kr analysis of silicate inclusions from iron meteorites. *Geochim. Cosmochim. Acta* **35**, 1231–1254.
- Bottke W. F., Richardson D. C., Michel P., and Love S. G. (1999) 1620 Geographos and 433 Eros: shaped by planetary tides. *Astron. J.* **117**, 1921–1928.
- Boyd F. R., and England J. L. (1965) The rhombic enstatite-clinoenstatite inversion. *Carnegie Inst. Washington, Ann. Rpt. Dir. Geophys. Lab.*, 117–120.
- Brandes E. A., and Brook G. B. (1998) *Smithells Metal Reference Book*, seventh ed. (with corrections). Butterworth-Heinemann, ca. 1600 pp.
- Brearley A. J., and Jones R. H. (1998) Chondritic meteorites. In *Planetary Materials*, vol. 36 (ed. J. J. Papike). Mineralogical Society of America, pp. 3-1–3-398.
- Brett R., and Sato M. (1984) Intrinsic oxygen fugacity measurements on seven chondrites, a pallasite, and a tektite and the redox state of meteorite parent bodies. *Geochim. Cosmochim. Acta* **58**, 111–120.
- Britt D. T., and Pieters C. M. (1991) Black ordinary chondrites: an analysis of abundance and fall frequency. *Meteoritics* **26**, 279–285.
- Britt D. T., Yeomans D., Housen K., and Consolmagno G. (2002) Asteroid density, porosity and structure. In *Asteroids III* (eds. W.F. Bottke, A. Cellino, P. Paolicchi and R. P. Binzel). Univ. Arizona Press, Tucson, pp. 485–500.
- Brownlee A. J., and Rajan R. S. (1973) Micrometeorite craters discovered on chondrule-like objects from Kapoeta meteorite. *Science* **182**, 1341–1344.
- Buening D. K., and Buseck P. R. (1973) Fe–Mg lattice diffusion in olivine. *J. Geophys. Res.* **78**, 6852–6862.
- Chakraborty S. (1997) Rates and mechanisms of Fe–Mg interdiffusion in olivine at 980°–1300 °C. *J. Geophys. Res.* **102**, 12317–12331.
- Chen M., Sharp T. G., ElGoresy A., Wopenka B., and Xie X. (1996) The majorite-pyrope + magnesiowüstite assemblage: Constraints on the history of shock veins in chondrites. *Science* **271**, 1570–1573.
- Cheng A. F., and Barnouin-Jha O. S. (1999) Giant craters on Mathilde. *Icarus* **140**, 34–48.
- Clayton R. N., and Mayeda T. K. (1996) Oxygen isotope studies of achondrites. *Geochim. Cosmochim. Acta* **60**, 1999–2017.
- Clayton R. N., and Mayeda T. K. (1999) Oxygen isotope studies of carbonaceous chondrites. *Geochim. Cosmochim. Acta* **63**, 2089–2104.
- Dixon E. T., Bogard D. D., Garrison D. H., and Rubin A. E. (2004)  $^{39}\text{Ar}$ – $^{40}\text{Ar}$  evidence for early impact events on the LL parent body. *Geochim. Cosmochim. Acta* **68**, 3779–3790.
- El Goresy A. (2006) Native copper in FeNi and the assemblage chromite-plagioclase in ordinary chondrites: discarded as shock parameters (abstract). Desert Meteorites Workshop. *Meteorit. Planet. Sci.* **41**(Supplement), A204.
- El Goresy A., Wadhwa M., Nagel H.-J., Zinner E. K., Janicke J., and Crozaz G. (1992)  $^{53}\text{Cr}$ – $^{53}\text{Mn}$  systematics of Mn-bearing sulfides in four enstatite chondrites (abstract). *Lunar Planet. Sci.* **23**, 331–332.
- El Goresy A., Zinner E., and Marti K. (1995) Survival of isotopically heterogeneous graphite in a differentiated meteorite. *Nature* **373**, 496–499.
- El Goresy A., Zinner E., Pellas P., and Caillet C. (2005) A menagerie of graphite morphologies in the Acapulco meteorite with diverse carbon and nitrogen isotopic signatures: implications for the evolution history of acapulcoite meteorites. *Geochim. Cosmochim. Acta* **69**, 4535–4556.
- Eugster O. (1988) Cosmic-ray production rates for  $^3\text{He}$ ,  $^{21}\text{Ne}$ ,  $^{38}\text{Ar}$ ,  $^{83}\text{Kr}$  and  $^{126}\text{Xe}$  in chondrites based on  $^{81}\text{Kr}$ –Kr exposure ages. *Geochim. Cosmochim. Acta* **52**, 1649–1662.
- Eugster O., and Lorenzetti S. (2005) Cosmic-ray exposure ages of four acapulcoites and two differentiated achondrites and

- evidence for a two-layer structure of the acapulcoite/lodranite parent asteroid. *Geochim. Cosmochim. Acta* **69**, 2675–2685.
- Fei Y., Zhang L., Komabayashi T., Sata N., and Bertka C. M. (2006) Evidences for a liquid martian core. *Lunar Planet. Sci.* **37**. Lunar Planet. Inst., Houston. #1500 (abstr.).
- Floss C. (2000) Complexities on the acapulcoite–lodranite parent body: evidence from trace element distributions in silicate minerals. *Meteorit. Planet. Sci.* **35**, 1073–1085.
- Freer R. (1981) Diffusion in silicate minerals and glasses: a data digest and guide to the literature. *Contrib. Mineral. Petrol.* **76**, 440–454.
- Gomes C. B., and Keil K. (1980) *Brazilian Stone Meteorites*. Univ. New Mexico, Albuquerque, 161 pp.
- Grady M. M. (2000) *Catalogue of Meteorites*, fifth ed. Cambridge University Press, Cambridge, United Kingdom.
- Grossman J. N. (2000) The Meteoritical Bulletin, No. 84, 2000 August. *Meteorit. Planet. Sci.* **35**, A199–A225.
- Grossman J. N., and Zipfel J. (2001) The Meteoritical Bulletin, No. 85, 2001 September. *Meteorit. Planet. Sci.* **36**, A293–A322.
- Grover J. E. (1972) The stability of low-clinoenstatite in the system  $Mg_2Si_2O_6$ – $CaMgSi_2O_6$  (abstract). *Trans. Am. Geophys. Union* **53**, 539.
- Hansen M. (1958) *Constitution of Binary Alloys*. McGraw-Hill, New York, 1305 pp.
- Heymann D. (1967) On the origin of hypersthene chondrites: ages and shock effects of black chondrites. *Icarus* **6**, 189–221.
- Hintenberger H., Schultz L., and Weber H. (1969) Rare gases in the iron and in the inclusions of the Campo del Cielo meteorite, El Taco. In *Meteorite Research* (ed. P. M. Millman). Reidel, pp. 895–900.
- Hornemann U., and Müller W. F. (1971) Shock-induced deformation twins in clinopyroxene. *Neues Jahrbuch Mineralogie* **6**, 247–256.
- Housen K. R., and Holsapple K. A. (1999) Impact cratering on porous low-density bodies. *Lunar Planet. Sci.* **30**. Lunar Planet. Inst., Houston. #1228 (abstr.).
- Huber H., Rubin A. E., and Wasson J. T. (2006) Bulk compositions and petrographic characteristics of ten unusual carbonaceous chondrites. *Lunar Planet. Sci.* **37**. Lunar Planet. Inst., Houston. #2381 (abstr.).
- Hutchison R. (2004) *Meteorites: A Petrologic, Chemical and Isotopic Synthesis*. Cambridge University Press, Cambridge, 506 pp.
- Jarosewich E. (1990) Chemical analyses of meteorites: a compilation of stony and iron meteorite analyses. *Meteoritics* **25**, 323–337.
- Jurewicz A. J. G., Mittlefehldt D. W., and Jones J. H. (1995) Experimental partial melting of the St. Severin (LL) and Lost City (H) chondrites. *Geochim. Cosmochim. Acta* **59**, 391–408.
- Kallemeyn G. W., and Wasson J. W. (1985) The compositional classification of chondrites: IV. Ungrouped chondritic meteorites and clasts. *Geochim. Cosmochim. Acta* **49**, 261–270.
- Kallemeyn G. W., Rubin A. E., and Wasson J. T. (1994) The compositional classification of chondrites: VI. The CR carbonaceous chondrite group. *Geochim. Cosmochim. Acta* **58**, 2873–2888.
- Keil K. (2000) Thermal alteration of asteroids: evidence from meteorites. *Planet. Space Sci.* **48**, 887–903.
- Keil K., Kurat G., Prinz M., and Green J. A. (1972) Lithic fragments, glasses and chondrules from Luna 16 fines. *Earth Planet. Sci. Lett.* **13**, 243–256.
- Keil K., Stöffler D., Love S. G., and Scott E. R. D. (1997) Constraints on the role of impact heating and melting in asteroids. *Meteorit. Planet. Sci.* **32**, 349–363.
- Kessel R., Beckett J. R., Huss G. R., and Stolper E. M. (2004) The activity of chromite in multicomponent spinels: Implications for T-fo<sub>2</sub> conditions of equilibrated H chondrites. *Meteorit. Planet. Sci.* **39**, 1287–1305.
- Kimura M., Tsuchiyama A., Fukuoka T., and Imura, Y. (1992) Antarctic primitive achondrites, Yamato-74025, -75300, and -75305: their mineralogy, thermal history and the relevance to winonaite. *Proc. NIPR Symp. Antarct. Met.* **5**, 165–190.
- Kojima H., and Imae N. (1998). *Meteorites News* **7**, 1–95.
- Kullerud G. (1963) The Fe–Ni–S system. *Carnegie Inst. Wash. Yrbk* **62**, 175–189.
- Kurat G., Keil K., Prinz M., and Nehru C. E. (1972). Chondrules of lunar origin. *Proc. Lunar Planet. Sci. Conf.* **3rd**, 707–721.
- Lambert P., Lewis C., and Moore C. B. (1984) Repeated shock and thermal metamorphism of the Abernathy meteorite. *Meteoritics* **19**, 29–48.
- Mason B., and Wiik H. B. (1962) The Renazzo meteorite. *Amer. Mus. Novitates* **2106**, 1–11.
- Mason B., and Wiik H. B. (1964) The amphoterites and meteorites of similar composition. *Geochim. Cosmochim. Acta* **28**, 533–538.
- McCoy T. J., Keil K., Clayton R. N., and Mayeda T. K. (1993) Classificational parameters for acapulcoites and lodranites: the cases of FRO 90011, EET 84302 and ALH A81187/84190 (abstract). *Lunar Planet. Sci.* **XXIV**, 945–946.
- McCoy T. J., Keil K., Clayton R. N., Mayeda T. K., Bogard D. D., Garrison D. H., Huss G. R., Hutcheon I. D., and Wieler R. (1996) A petrologic, chemical, and isotopic study of Monument Draw and comparison with other acapulcoites: evidence for formation by incipient partial melting. *Geochim. Cosmochim. Acta* **60**, 2681–2708.
- McCoy T. J., Keil K., Clayton R. N., Mayeda T. K., Bogard D. D., Garrison D. H., and Wieler R. (1997a) A petrologic and isotopic study of lodranites: evidence for early formation as partial melt residues from heterogeneous precursors. *Geochim. Cosmochim. Acta* **61**, 623–637.
- McCoy T. J., Keil K., Muenow D. W., and Wilson L. (1997b) Partial melting and melt migration in the acapulcoite–lodranite parent body. *Geochim. Cosmochim. Acta* **61**, 639–650.
- McSween H. Y., and Labotka T. C. (1993) Oxidation during metamorphism of the ordinary chondrites. *Geochim. Cosmochim. Acta* **57**, 1105–1114.
- McSween H. Y., Ghosh A., Grimm R. E., Wilson L., and Young E. D. (2002) Thermal evolution models of asteroids. In *Asteroids III* (eds. W. F. Bottke, A. Cellino, P. Paolicchi and R. P. Binzel). University of Arizona Press, pp. 559–571.
- Melosh H. J. (1989) *Impact Cratering: A Geologic Process*. Oxford University Press, New York, 245 pp.
- Min K., Farley K. A., Renne P. R., and Marti K. (2003) Single grain (U–Th)/He ages from phosphates in Acapulco meteorite and implications for thermal history. *Earth Planet. Sci. Lett.* **209**, 323–336.
- Mittlefehldt D. W. (1990) Petrogenesis of mesosiderites: I. Origin of mafic lithologies and comparison with basaltic achondrites. *Geochim. Cosmochim. Acta* **54**, 1165–1173.
- Mittlefehldt D. W., and Lindstrom M. M. (2001) Petrology and geochemistry of Patuxent Range 91501, a clast-poor impact melt from the L-chondrite parent body and Lewis Cliff 88663, an L7 chondrite. *Meteorit. Planet. Sci.* **36**, 439–457.
- Mittlefehldt D. W., Lindstrom M. M., Bogard D. D., Garrison D. H., and Field S. W. (1996) Acapulco- and Lodran-like achondrites: petrology, geochemistry, chronology, and origin. *Geochim. Cosmochim. Acta* **60**, 867–882.
- Moggi-Cecchi V., Bindi L., and Pratesi G. (2005) A new iron-nickel phosphide from the Northwest Africa 1054 meteorite (abstract). *Meteorit. Planet. Sci.* **40**, A105.
- Molin G. M., Domeneghetti M. C., Salviulo G., Stimpfl M., and Tribaudino M. (1994) Antarctic FRO90011 lodranite: cooling

- history from pyroxene crystal chemistry and microstructure. *Earth Planet. Sci. Lett.* **128**, 479–487.
- Nagahara H. (1992) Yamato-8002: partial melting residue on the “unique” chondrite parent body. *Proc. NIPR Symp. Antarct. Met.* **5**, 191–223.
- Palme H., Schultz L., Spettel B., Weber H. W., Wänke H., Michel-Levy M. C., and Lorin J. C. (1981) The Acapulco meteorite: chemistry, mineralogy and irradiation effects. *Geochim. Cosmochim. Acta* **45**, 727–752.
- Patzert A., Hill D. H., and Boynton W. V. (2004) Evolution and classification of acapulcoites and lodranites from a chemical point of view. *Meteorit. Planet. Sci.* **39**, 61–85.
- Pellas P., Fiéni C., Trieloff M., and Jessberger E. K. (1997) The cooling history of the Acapulco meteorite as recorded by the  $^{244}\text{Pu}$  and  $^{40}\text{Ar}$ – $^{39}\text{Ar}$  chronometers. *Geochim. Cosmochim. Acta* **61**, 3477–3501.
- Prinz M., Waggoner D. G., and Hamilton P. J. (1980) Winonaites: a primitive achondritic group related to silicate inclusions in IAB irons (abstract). *Lunar Planet. Sci.* **XI**, 902–904.
- Prinz M., Nehru C. E., Delaney J. S., and Weisberg M. (1983) Silicates in IAB and IIICD irons, winonaites, lodranites, and Brachina: a primitive and a modified-primitive group (abstract). *Lunar Planet. Sci.* **XIV**, 616–617.
- Raikes S. A., and Ahrens T. S. (1979) Post-shock temperatures in minerals. *Geophys. J. Roy. Astron. Soc.* **58**, 717–747.
- Ramdohr P. (1973) *The Opaque Minerals in Stony Meteorites*. Elsevier, Amsterdam, 245 pp.
- Ramdohr P. (1980) *The Ore Minerals and their Intergrowths*, second ed. Pergamon Press, Oxford, 1207 pp.
- Rubin A. E. (1983) The Adhi Kot breccia and its implications for the origin of chondrules and silica-rich clasts in enstatite chondrites. *Earth Planet. Sci. Lett.* **64**, 201–212.
- Rubin A. E. (1992) A shock-metamorphic model for silicate darkening and compositionally variable plagioclase in CK and ordinary chondrites. *Geochim. Cosmochim. Acta* **56**, 1705–1714.
- Rubin A. E. (1994) Metallic copper in ordinary chondrites. *Meteoritics* **29**, 93–98.
- Rubin A. E. (2000) Petrologic, geochemical and experimental constraints on models of chondrule formation. *Earth-Sci. Rev.* **50**, 3–27.
- Rubin A. E. (2002) Post-shock annealing of MIL99301 (LL6): implications for impact heating of ordinary chondrites. *Geochim. Cosmochim. Acta* **66**, 3327–3337.
- Rubin A. E. (2003) Chromite–plagioclase assemblages as a new shock indicator; Implications for the shock and thermal histories of ordinary chondrites. *Geochim. Cosmochim. Acta* **67**, 2695–2709.
- Rubin A. E. (2004) Post-shock annealing and post-annealing shock in equilibrated ordinary chondrites: implications for the thermal and shock histories of chondritic asteroids. *Geochim. Cosmochim. Acta* **68**, 673–689.
- Rubin A. E. (2006) Shock, post-shock annealing and post-annealing shock in ureilites. *Meteorit. Planet. Sci.* **41**, 125–133.
- Rubin A. E., and Grossman J. N. (1985) Phosphate-sulfide assemblages and Al/Ca ratios in type-3 chondrites. *Meteoritics* **20**, 479–489.
- Rubin A. E., and Jones R. H. (2003) Spade: an H-chondrite impact-melt breccia that experienced post-shock annealing. *Meteorit. Planet. Sci.* **38**, 1507–1520.
- Rubin A. E., and Keil K. (1983) Mineralogy and petrology of the Abee enstatite chondrite breccia and its dark inclusions. *Earth Planet. Sci. Lett.* **62**, 118–131.
- Rubin A. E., and Scott E. R. D. (1997) Abee and related EH chondrite impact-melt breccias. *Geochim. Cosmochim. Acta* **61**, 425–435.
- Rubin A. E., Scott E. R. D., Taylor G. J., Keil K., Allen J. S. B., Mayeda T. K., Clayton R. N., and Bogard D. D. (1983) Nature of the H chondrite parent body regolith: evidence from the Dimmitt breccia. *Lunar Planet. Sci. Conf.* **13th**, A741–A754.
- Rubin A. E., Scott E. R. D., and Keil K. (1997) Shock metamorphism of enstatite chondrites. *Geochim. Cosmochim. Acta* **61**, 847–858.
- Rubin A. E., Ulff-Møller F., Wasson J. T., and Carlson W. D. (2001) The Portales Valley meteorite breccia: evidence for impact-induced melting and metamorphism of an ordinary chondrite. *Geochim. Cosmochim. Acta* **65**, 323–342.
- Rubin A. E., Kallemeyn G. W., and Wasson J. T. (2002) A IAB-complex iron meteorite containing low-Ca clinopyroxene: Northwest Africa 468 and its relationship to lodranites and formation by impact melting. *Geochim. Cosmochim. Acta* **66**, 3657–3671.
- Rumble D., Irving A. J., Bunch T. E., Wittke J. H., and Kuehner S. M. (2005) Discrimination of acapulcoites and lodranites from winonaites (abstract). *Meteorit. Planet. Sci.* **40**, A133.
- Russell S. S., Zolensky M., Righter K., Folco L., Jones R., Connolly H. C., Grady M. M., and Grossman J. N. (2005) The Meteoritical Bulletin, No. 89, 2005 September. *Meteorit. Planet. Sci.* **40**, A201–A263.
- Ruzicka A., Snyder G. A., and Taylor L. A. (2000) Crystal-bearing lunar spherules: impact melting of the Moon’s crust and implications for the origin of meteoritic chondrules. *Meteorit. Planet. Sci.* **35**, 173–192.
- Sack R. O., and Ghiorso M. S. (1991). Chromite as a petrogenetic indicator. *Rev. Mineral.* **25**, 323–353, In *Oxide Minerals: Petrologic and Magnetic Significance* (ed. D. H. Lindsley). Mineralogical Society of America, BookCrafters, Chelsea, Michigan.
- Scherer P., and Schultz L. (2000) Noble gas record, collisional history, and pairing of CV, CO, CK, and other carbonaceous chondrites. *Meteorit. Planet. Sci.* **35**, 145–153.
- Schmitt R. T., Deutsch A., and Stöffler D. (1993) Shock effects in experimentally shocked samples of the H6 chondrite Kernouvé (abstract). *Meteoritics* **28**, 431–432.
- Schultz L., and Kruse H. (1989) Helium, neon, and argon in meteorites – a data compilation. *Meteoritics* **24**, 155–172.
- Schultz L., Palme H., Spettel B., Weber H. W., Wänke H., Christophe Michel-Levy M., and Lorin J. C. (1982) Allan Hills 77081 – an unusual stony meteorite. *Earth Planet. Sci. Lett.* **61**, 23–31.
- Scott E. R. D. (1982) Origin of rapidly solidified metal–troilite grains in chondrites and iron meteorites. *Geochim. Cosmochim. Acta* **46**, 813–823.
- Signer P., and Suess H. E. (1963) Rare gases in the sun, in the atmosphere, and in meteorites. In *Earth Science and Meteoritics* (eds. J. Geiss and E. D. Goldberg). North-Holland, Amsterdam, pp. 241–272.
- Smith B. A., and Goldstein J. I. (1977) The metallic microstructures and thermal histories of severely reheated chondrites. *Geochim. Cosmochim. Acta* **41**, 1061–1072.
- Speich G. R., and Swann P. R. (1965) Yield strength and transformation substructure of quenched iron-nickel alloys. *J. Iron Steel Inst.* **203**, 480–485.
- Stewart S. T., and Ahrens T. J. (1999) Porosity effects on impact processes in solar system materials. *Lunar Planet. Sci.* **30**, #2020 (abstr.).
- Stöffler D., Keil K., and Scott E. R. D. (1991) Shock metamorphism of ordinary chondrites. *Geochim. Cosmochim. Acta* **55**, 3845–3867.
- Swindle T. D., Kring, D. A., Olson E. K., and Isachsen C.E. (2006) Ar–Ar dating of shock-melted ordinary chondrites: chronology

- of asteroidal impacts. *Lunar Planet. Sci.* 37. Lunar Planet. Inst., Houston. #1454 (abstr.).
- Symes S. J. K., Sears D. W. G., Akridge D. G., Huang S., and Benoit P. H. (1998) The crystalline lunar spherules: their formation and implications for the origin of meteoritic chondrules. *Meteorit. Planet. Sci.* **33**, 13–29.
- Taylor G. J., and Heymann D. (1971) Postshock thermal histories of reheated chondrites. *J. Geophys. Res.* **76**, 1879–1893.
- Van Schmus W. R., and Ribbe P. H. (1968) The composition and structural state of feldspar from chondritic meteorites. *Geochim. Cosmochim. Acta* **32**, 1327–1342.
- Veverka J., Thomas P., Harch A., Clark B., Bell, III, J. F., Carcich B., Joseph J., Murchie S., Izenberg N., Chapman C., Merline W., Malin M., McFadden L., and Robinson M. (1999) NEAR encounter with asteroid 253 Mathilde: overview. *Icarus* **140**, 3–16.
- Wasson J. T. (1985) *Meteorites: Their Record of Early Solar System History*. Freeman, 267 pp.
- Wasson J. T., and Kallemeyn G. W. (1988) Compositions of chondrites. *Philos. Trans. R. Soc. Lond.* **A325**, 535–544.
- Weisberg M. K., and Prinz M. (2000) The Grosvenor Mountains 95577 CR1 chondrite and hydration of the CR chondrites (abstract). *Meteorit. Planet. Sci.* **35**, A168.
- Weisberg M. K., Prinz M., Clayton R. N., and Mayeda T. K. (1993) The CR (Renazzo-type) carbonaceous chondrite group and its implications. *Geochim. Cosmochim. Acta* **57**, 1567–1586.
- Wilson A. H. (1982) The geology of the Great ‘Dyke’, Zimbabwe: the ultramafic rocks. *J. Petrol.* **23**, 240–292.
- Yanai K. (2001) Lodranites and their subgroups related with some acapulcoite. *Lunar Planet. Sci.* 32. #1665 (abstr.).
- Yanai K., and Kojima H. (1991) Yamato-74063: chondritic meteorite classified between E and H chondrite groups. *Proc. NIPR Symp. Antarct. Met.* **4**, 118–130.
- Young E. D., Nagahara H., Mysen B. O., and Audet D. M. (1998) Non-Rayleigh oxygen isotope fractionation by mineral evaporation: theory and experiments in the system SiO<sub>2</sub>. *Geochim. Cosmochim. Acta* **62**, 3109–3116.
- Yugami K., Miyamoto M., Takeda H., and Hiroi T. (1993) Mineralogy of ALH81187: a partly reduced acapulcoite (abstract). *Papers Presented to the 18th Symp. Antarc. Met.*, 34–37.
- Zema M., Domeneghetti M. C., and Molin G. M. (1996) Thermal history of Acapulco and ALHA81261 acapulcoites constrained by Fe<sup>2+</sup>–Mg ordering in orthopyroxene. *Earth Planet Sci. Lett.* **144**, 359–367.
- Zipfel J., Palme H., Kennedy A. K., and Hutcheon I. D. (1995) Chemical composition and origin of the Acapulco meteorite. *Geochim. Cosmochim. Acta* **59**, 3607–3627.

Associate editor: Alexander N. Krot